CHALMERS
UNIVERSITY OF TECHNOLOGY

Towards Optimizing Acetic Acid Utilization In *Saccharomyces cerevisiae* Through gRNA-Landing Pads

Master's thesis in Biotechnology

ERIK BERG

DEPARTMENT OF LIFE SCIENCES

CHALMERS UNIVERSITY OF TECHNOLOGY
Gothenburg, Sweden 2024
www.chalmers.se

MASTER'S THESIS 2024

Towards Optimizing Acetic Acid Utilization in *Saccharomyces Cerevisiae* through gRNA-Landing Pads

MASTER'S THESIS

ERIK BERG
June 17, 2024

CHALMERS
UNIVERSITY OF TECHNOLOGY

Department of Life Sciences
Division of Industrial Biotechnology
CHALMERS UNIVERSITY OF TECHNOLOGY
Gothenburg, Sweden 2024

Towards Optimizing Acetic Acid Utilization in *S. cerevisiae* through gRNA-Landing Pads

ERIK BERG

Supervisor: Arne Peetermans
Examiner: Yvonne Nygård

Master's Thesis 2024
Department of Life Sciences
Division of Industrial Biotechnology
Nygård Group
Chalmers University of Technology
SE-412 96 Gothenburg
Telephone +46 76 035 7181

Typeset in LaTeX
Gothenburg, Sweden 2024

Abstract

Lignocellulosic biomass, residual biomass from the agricultural and forestry industries, is the most abundant organic substance on the planet. For efficient utilization by *Saccharomyces cerevisiae*, the biomass must undergo a pretreatment process that typically generates strong inhibitors, with acetate being the most prominent. This project served as a proof of concept and explored optimization of acetate utilization in *Saccharomyces cerevisiae* using a gRNA-landing pad strategy. This was done through a wide range of molecular biology methods such as the transformation of *Escherichia coli* and the *Saccharomyces cerevisiae* strain LX6, restriction cloning, cloning using the MoClo system, as well as in-silico design of plasmids and primers. A gRNA-landing pad was successfully assembled in-vitro, using in-silico custom-made MoClo parts, and transformed into *Escherichia coli*. Transformation of the gRNA-landing pad into LX6 presented a challenge, that as of yet is not overcome. Despite the challenges in transforming the yeast, the creation of an easy-to-assemble gRNA-landing pad could enable a fast and reliable method for future research involving gRNA-landing pads *Saccharomyces cerevisiae*.

Acknowledgements

I would like to thank my examiner Assoc. Prof. Yvonne Nygård for giving me the opportunity to work on this project, which has proven both challenging and intriguing as well as supplying me with much-needed lab experience. I would also like to thank my supervisor Dr. Arne Peetermans for providing me with guidance and assistance during the various stages of this project. A big thanks goes out to everyone at the division of industrial biotechnology for helping me in the lab and providing a friendly work environment. Finally, I would like to extend my gratitude to all my friends and family for supporting me not only during this project but throughout my entire journey through university – and what a journey it has been.

Contents

1

Introduction

1.1 Lignocellulosic biomass utlization

Lignocellulosic biomass, a residue from the agricultural and forestry industries, is the most abundant organic substance on the planet [1]. The competent microorganism *S. cerevisiae* has already been engineered to utilize lignocellulosic biomass, although this utilization has not yet been optimized [2]. Due to *S. cerevisiae's* vast area of applications, including the food industry, cosmetics, pharmaceuticals, and chemical production, there is a growing interest both within academia and industry to further improve upon its utlization of the abundant feedstock; lignocellulosic biomass [3][4].

Lignocellulosic biomass belongs to the category "second-generation feedstock", as opposed to first-generation feedstock. While first-generation feedstock is made up of biomass such as corn, wheat and grains, all of which are considered edible for humans - second-generation feedstocks are not suitable for consumption [5]. Using second-generation feedstock can therefore be considered advantageous as it does not cause the same competition between the food industry and bio-based industries such as the bio-fuels industry [6]. Other than the food security issue the supposed environmental benefits from using first-generation feedstock compared to fossil fuels, partly due to deforestation and impact of nitrogen fertilizers, is in of itself in question [7]. The use of the more environmentally friendly second-generation feedstock, lignocellulosic biomass, can therefore be considered a front-runner candidate in the race to find a sustainable feedstock.

Lignocellulosic biomass' composition depends on what plant it is derived from. However, it tends to be composed of 35-70 wt% cellulose, 20-40 wt% hemicellulose, and 5-25wt% lignin [8]. In its raw form, lignocellulosic biomass is notoriously difficult to utilize - it tends to require pretreatment for efficient use by microorganisms such as *S. cerevisiae* [9]. Pretreatment of lignocellulosic biomass creates slurry of a vast range of sugars and other compounds, some of which exercise inhibitory properties upon *S. cerevisiae* - this resulting biomass is known as lignocellulosic hydrolysate [9][10]. One of these by-products that are created in the pre-treatment of lignocellulosic hydrolysate is the powerful inhibitor acetic acid; however, many different inhibitory sugars and compounds such as, glucose, xylose, arabinose and pentoses are also formed. [11].

1.2 Acetic acid and *S. cerevisiae*

1.2.1 Acetic acid Tolerance

In lignocellulistic hydrolysates concentration of acetic acid can reach as high as 11.5 g/L (192 mM) at which point the yeast's physiology is strongly effected [12] [13]. *S. cerevisiae* which has been exposed to acetic acid may stop proliferation, and never resume it. The fraction of *S. cerevisiae* which exhibit this behavior has been shown to be directly dependent on the acetic acid concentration, as well as the strains' genetic composition [14]. Improving tolerance of acetic acid in *S. cerevisiae* through genetically modifying the yeast, which would reduce the concentration of said acid, could therefore lessen the fraction of *S. cerevisiae* exhibiting no proliferation. Other than its direct effect on cell

proliferation acetic acid may also inhibit the cell's glucose consumption and cause oxidative damage [11].

Improving the tolerance of acetic acid in *S. cerevisiae* through genetic manipulation has since long been a goal when it comes to optimizing production using lignocellulosic hydrolysates as a feedstock. Overexpression of acetic acid transporters have been identified as one such target which can improve a strains' tolerance [15]. Other areas frequently targeted is the plasma membrane of the yeast, which structure affects the permeability of acetic acid [11], and up-regulation of enzymes capable of converting acetic acid to other biomolecules [16]. However, previous omics studies have concluded that *S. cerevisiae's* tolerance to acetic acid lies under the control of a complex network of multi-functional genes, encoding for proteins which act in several different metabolic pathways [11]. This makes adapting the tolerance to acetic acid a difficult and multifaceted issue. While improving *S. cerevisiae's* tolerance to acetic acid is still an important goal, this study instead opts to improve its *utilization* - intending to provide an alternative, relatively unexplored approach. Here, several genes whose knock-out could potentially improve *S. cerevisiae's* vitality in lignocellulosic hydrolysate-media through acetic acid utilization have been identified.

1.2.2 Genes involved in acetic acid tolerance

ALD5 is a gene encoding for the expression of a member of the acetaldehyde dehydrogenase family - a family of enzymes with the essential function of catalyzing the conversion of acetaldehyde to acetate. In a previous study by Saint-Prix et al., knock-outs of all different members of the acetaldehyde dehydrogenase family were investigated, with *ALD5* and *ALD6* seemingly having the largest impact on acetate production [17]. Since *ALD6* is already deleted in the LX6 strain (see section 1.6, 'The LX6 strain') *ALD5* appears to be an appropriate target. The same study also investigated the effect on acetate production from the double-deletions of *ald6ald4*Δ and *ald6ald5*Δ - concluding that the double-deletion *ald6ald5*Δ has a larger effect on acetate production than the double-deletion *ald6ald4*Δ, and than each individual deletion. This double-deletion also displayed a negligible effect on cell growth. The effect on acetate production from the deletion of *ALD5* has previously not been investigated in many studies, the aforementioned study by Saint-Prix et al., is the only study listed in the SGD database where this was examined [18]. Due to the study's highly relevant double-deletion analysis and data clearly supporting that deletion of *ALD5* leads to a reduction in acetate production, its findings further corroborate that deletion of *ALD5* could be suitable. *ALD5* was thus chosen as a deletion-target.

Hexokinase II (HXK2) is an enzyme with a central role in the glucose metabolism and glucose repression in *S. cerevisiae*. Its deletion has been associated with earlier co-consumption of alternate carbon sources, such as acetic acid. Studies have shown that the deletion of *HXK2* leads to increased growth in high-glucose conditions, as well as an increased accumulation of pyruvate [19]. As mentioned before, many sugars which act as inhibitors in *S. cerevisiae* are created as by-products during the pretreatment process. Since *S. cerevisiae* during anaerobic conditions tends to prefer to utilize glucose, other carbon sources such as acetic acid, xylose and arabinose are left for a later fermentation phase - the latter may accumulate and cause stress in the cells. In another study the authors found that the deletion of *HXK2* leads to *S. cerevisiae* co-utilizing these sugars earlier on in the fermentation process [20]. Since the aforementioned sugars and acetic acid have inhibitory properties on *S. cerevisiae*, deleting *HXK2* and therefore promoting the co-utilization of these substrates should improve the strains' vitality in lignocellulosic hydrolysates. While the exact mechanisms behind *HXK2* are as of yet not known, it is believed that it during the presence of glucose represses the expression of genes involved in catabolsm of alternative carbon sources. On a final note; during the transitional phase from utilization of primarily glucose, to other substrates - the diauxic shift - a bio-energetic 'valley of death' causes persistent problems as the cells during this transitional phase are stressed by the accumulation of toxic metabolites [21]. By co-consumption of different substrates in an earlier phase this may be avoided -

something which is of especially great interest in lignocellulosic hydrolysate-media where acetic acid already causes problems for *S. cerevisiae* [20].

Glyoxylate reductase (GOR1) is an enzyme which converts the toxic glyoxylate to glycolate, consuming NADPH in the process [22]. GOR1 is however not necessary for consumption of glyoxylate as there are several other enzymes that also facilitate its consumption, some of which are in the glyoxylate shunt, a pathway very much related to the TCA cycle, see Figure 1. The glyoxylate shunt is of interest for acetic acid utilization as the cycle involves acetyl-CoA, which in turn can be produced by acetic acid. In one study it was found that deletion of *GOR1* leads to a significant increase in biomass accumulation after *S. cerevisiae* has reached the diauxic shift, further corroborating the theory that deletion of *GOR1* could have desirable effects. In the same study the authors argue that the reason for this improved cell growth could be due to more NADPH being freed up for other cellular processes [23]. Within the glyoxylate shunt the conversion of glyoxylate to malate uses up acetyl-CoA in the process. By removing GOR1 more of the flux from glyoxylate could be directed towards malate, which subsequentely increases the acetyl-CoA consumption. Since acetyl-CoA is created by conversion of acetate, this newly generated demand for acetyl-CoA could shift the flux to from acetate to acetyl-CoA. While GOR1 remains relatively unexplored, deletion of ICL1 has been explored. In one study the authors found the strains' where ICL1 had been deleted could not utilize acetate for growth [24]. Theoretically this could be due to less glyoxylate being created, which then leads to less malate formation and subsequently less acetyl-CoA being consumed - this would drive the flux from acetyl-CoA towards acetate. Deletion of *GOR1* would allow more flux to be directed through ICL1, consuming acetate in the process. Due to *GOR1's* involvement in the glyoxylate shunt, studies indicating improved growth upon its deletion, and its role as a significant NADPH sink, especialy under stress conditions [22], its deletion presents an intriguing target.

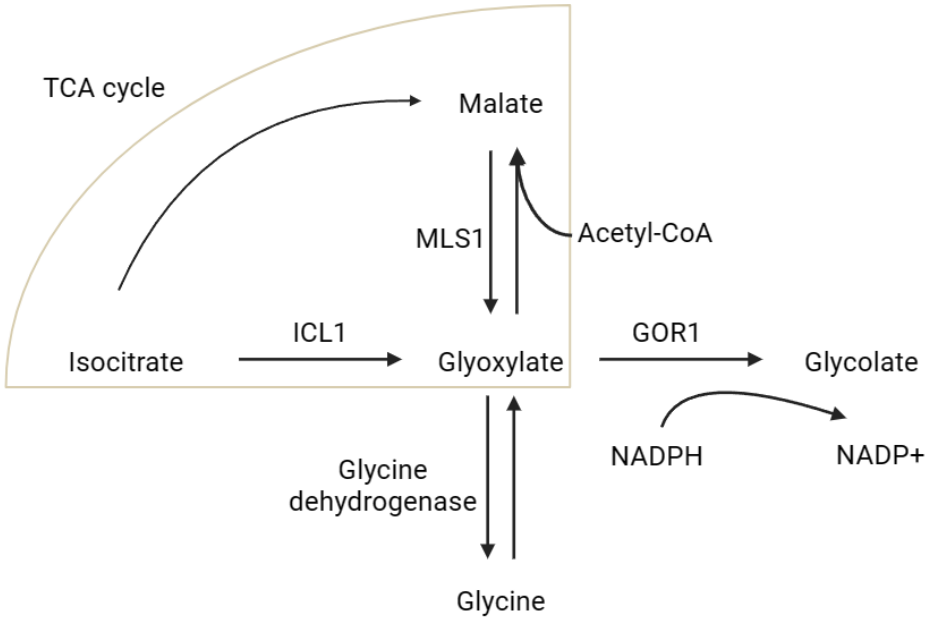

Figure 1: Glyoxylate metabolism in in *S. cerevisiae*

1.3 CRISPR and Multiplexing

1.3.1 Introduction to CRISPR gene editing

Clustered regularly interspaced palindromic repeats (CRISPR) gene-editing, is a technique for editing the genome of a living organism. It is based on the immune system found in many bacteria which protects them against viruses. CRISPR associated proteins (Cas) can through the use of so-called CRISPR-assosciated RNA (crRNA) and trans-activation CRISPR RNA (tracrRNA) bind to a target genetic sequence and cause a double-strand break. This double-strand break is inflicted where the target sequence is complimentary to the aforementioned crRNA. While the crRNA decides where Cas should inflict a double-strand break, the sgRNA which is connected to the tracrRNA forms a hairpin structure which provides stability to the complex [25]. This is illustrated for a Cas9 enzyme in figure 2. Through the creation of these double-strand breaks genetic material can be integrated in the genome of the target organism. The most commonly used Cas-enzyme is Cas9, but there are many other Cas enzymes which can be used for genetically engineering organisms. There are variations in how the different Cas enzymes work which can lead to some of the enzymes being more suitable for different tasks than others.

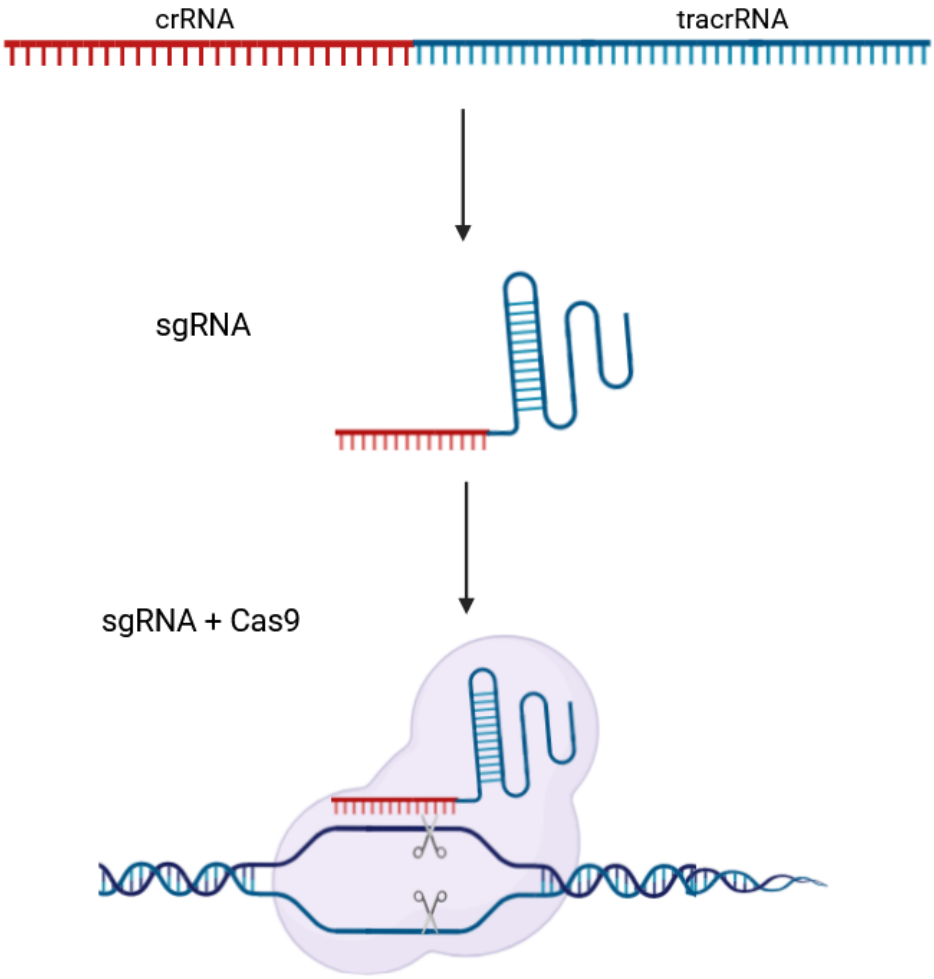

Figure 2: How crRNA, tracrRNA and Cas9 make up the CRISPR-Cas9 system.

1.3.2 Comparison of Cas9 and Cas12

CRISPR-Cas9 systems are at this point in time well-established as a valuable toolkit within molecular biology and genetics. While in general efficiently utilized, the CRISPR-Cas9 system is not without its drawbacks - perhaps the largest one being the inherent cytotoxicity of Cas9 in certain microorganisms [26] [27]. When using 'multiplexing', that is; targeting multiple loci in *S. cerevisiae* at the same time using different gRNAs there is a potential risk that this might accentuate these toxic effects, as the double-strand breaks (DSBs) caused by CRISPR systems in of themselves are toxic [28]. In this regard the more recently discovered CRISPR-Cas12 system poses as a promising alternative. The same inherent cytotoxic effects that are present in Cas9-based systems have not yet been observed in Cas12. Furthermore, Cas12 has a lower off-target genome editing than Cas9, due to it having a 'TTTV' PAM site whereas Cas9 has a 'NGG'[29]. Cas9 requires a crRNA and a tracrRNA, which together form the sgRNA. Whereas Cas12 only requires a crRNA, this crRNA is however referred to as 'sgRNA' in Cas12 systems. As Cas12 only requires a crRNA these can easily be assembled into an array which facilitates multiplexing, such an array in Cas9-system needs to be a lot larger, making it less ideal. Another advantage of using Cas12 over Cas9 is that the type of double-strand break that is caused by Cas12 creates sticky ends, whereas Cas9 generates blunt ends, see Figure 3. Sticky ends are less prone to facilitate non-homologous end joining, which can cause indel mutations. If an indel mutation occurs at a cleavage site this will in turn make the sgRNA unable to bind to the DNA, which results in an unintended indel mutation. Because Cas12 double-strand breaks do not facilitate indel mutations, the CRISPR-Cas12 complex can in case of self-ligation, recut the target loci until the another cellular repair mechanism - homology-directed repair - facilitates uptake of the desired donor DNA. [30]

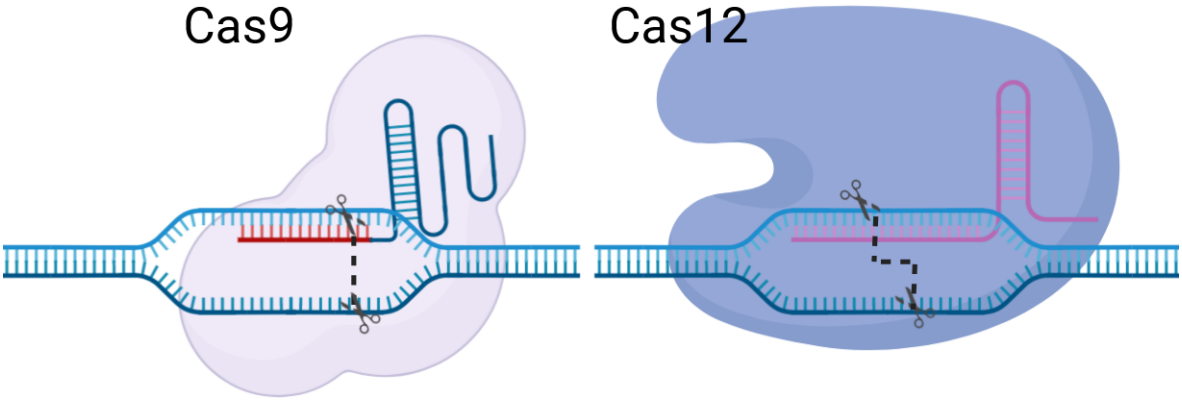

Figure 3: Schematic illustration showing how Cas9 vs Cas12 creates blunt and sticky ends respectively.

1.3.3 Different strategies for multiplexing using Cas12

Different strategies for supplying Cas12 with sgRNA for multiplexing have previously been investigated. The 'sgRNA-array' method involves delivering sgRNAs in a continuous array, relying on Cas12's ability to process the array into individual sgRNAs [31]. The conventional, or 'dispersed sgRNA' method, involves delivering the sgRNAs separate just as is done for Cas9. Previous research is inconclusive as to what method is the most efficient [31] [32]. Both methods involve restricting the sequence encoding the expression of the Cas12 complex from its vector plasmid. This is done to more accurately control the expression of the Cas12 enzyme, compared to transformations using the vector plasmid. Another angle is that by not using the circular vector plasmid there is no risk of *S. cerevisiae* taking up said plasmid. An unintended transformation of *S. cerevisiae* using the vector plasmid leads to prolonged Cas12 expression and therefore increases the risk of off-target double-strand breaks, this has been identified as a problem in plasmids expressing Cas9 [33].

1.4 Introduction to the acetic acid biosensor

The biosensor, pMM4_14, which has previously been developed by Mormino et al [34] contains two different fluorescent markers: *mTurqouise2* and *mCherry2*. These two fluorescent markers together make up the acetic acid biosensor through their difference in expression levels depending on the concentration of acetic acid. The biosensor is flanked by *HO* homology arms for integration in said region, contains a geneticin resistance marker, and also contains *URA3*. These components of the biosensor are arranged in the order indicated in figure 4.

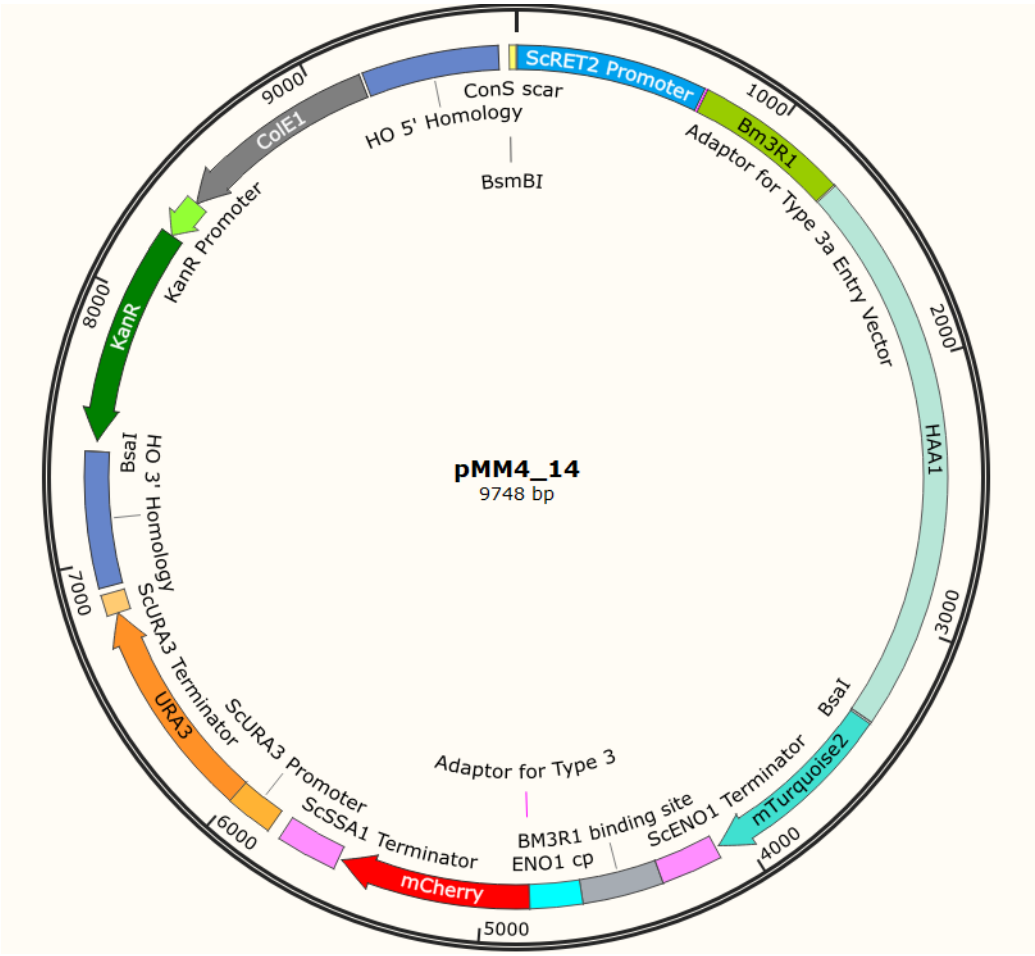

Figure 4: The acetic acid plasmid biosensor pMM4_14, as seen in SnapGene.

On one end of the biosensor the expression of *mTurquoise2*, coupled to *HAA1* and *Bm3R1*, is encoded. *HAA1* is a transcription factor, which when exposed to weak acids such as acetic acid, translocates to the nucleus from the cytosol [35]. This means that when *Bm3R1-HAA1-mTurquoise2* is expressed in the presence of acetic acid, the entire construct is transported to the nucleus. *Bm3R1* is a bacterial protein, which in the nucleus can bind to DNA, and thus induce expression of reporter genes. The *Bm3R1-HAA1-mTurquoise2*-construct is expressed by the *RET2* promoter, a constitutive which had previously been shown to exhibit the greatest dynamic range when compared to other promoters - stronger promoters are a less suitable choice as they result in "faster reporter saturation even at 0 mM acetic acid, or in poor expression of the reporter [34]."

mCherry2's expression lies under control of the *ENO1* core promoter (*ENO1cp)*. The *ENO1cp* contains

binding sites for BM3R1 which induce the expression of the underlying reporter gene. Expression of *BM3R1-HAA1-mTurquoise2* in the presence of acid is therefore directly coupled to the expression of *mCherry*. This means that in cellular stress-inducing low pH-conditions, such as those encountered in lignocellulosic hydrolysates, more *mCherry* should be expressed when compared to normal conditions. Figure 5 illustrates the components of the *mTurquoise2* and *mCherry2* part of the biosensor, as well as how the *Bm3R1-HAA1-mTurquoise2*-construct induces expression of *mCherry2*.

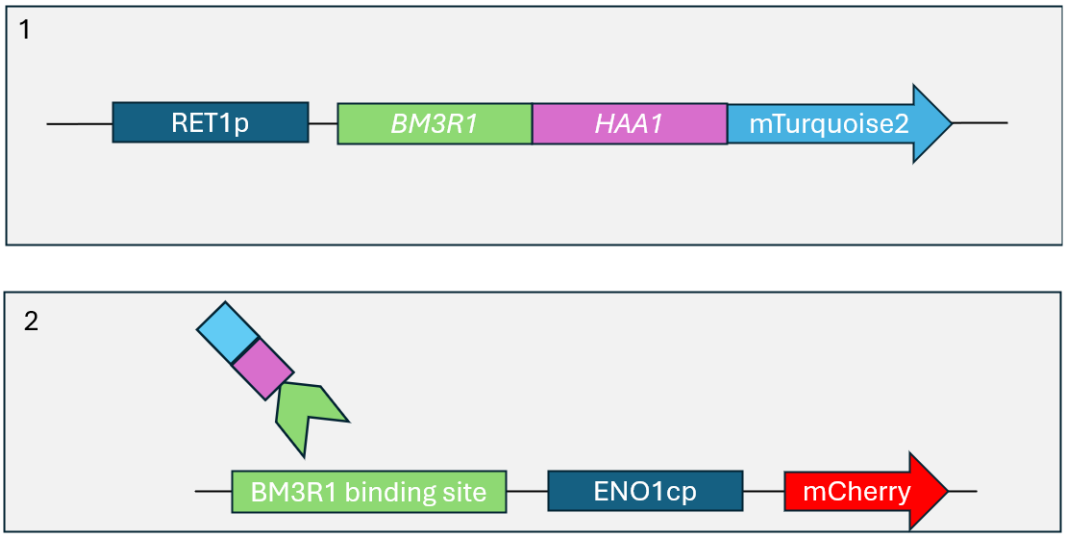

Figure 5: Illustration of the two fluorescent markers in the acetic acid biosensor, as well how the *Bm3R1-HAA1-mTurquoise2*-construct induces expression of *mCherry2*.

1.5 The MoClo system

MoClo is a modular cloning system that can be used to assemble multiple DNA parts from different plasmids into functional multigene constructs. The MoClo system utilizes type IIS restriction enzymes, which can restrict DNA outside of their recognition site, to create DNA fragments with compatible ends. Large libraries of plasmids containing a DNA sequence which is flanked by the type IIS restriction enzyme 'BsaI' have been created. These plasmids form the basis of the system and are known as 'level 0 modules'. Within the level 0 modules the plasmids can be further categorized into different 'parts', going all the way from part 1 plasmids, to part 8 plasmids. Upon restriction by type IIS restriction enzymes, part 5 plasmids, for example, will be cleaved into a backbone and a DNA part. This DNA part has sticky ends which are compatible with the sticky ends created by type IIS restriction enzymes restricting part 4, on its 5' end overhang, and part 6 on its 3' end overhang. This makes it possible for the DNA parts to anneal and form an array of parts 4 to 6, see figure 6. Of course, the same principle applies to every single MoClo part from 1 to 8 - giving access to an easy way of stitching together different DNA segments to form complex constructs. Each type part only has overhangs which are compatible with consecutive type parts - meaning that a type 7 part, for example, is not compatible with a type 3 part.

1.6 The LX6 strain

The *S. cerevisiae* strain LX6, developed by Choi et al., [36] was created with the goal of improving its acetate utlization. LX6 is a segregant from the strain CEN.PK XXX, which has had its xylose-utlization improved [37]. It features some prominent engineered features, the most important in regards to optimizing acetate utlization being the deletion of *ALD6*. *ALD6* is one of the five members of the

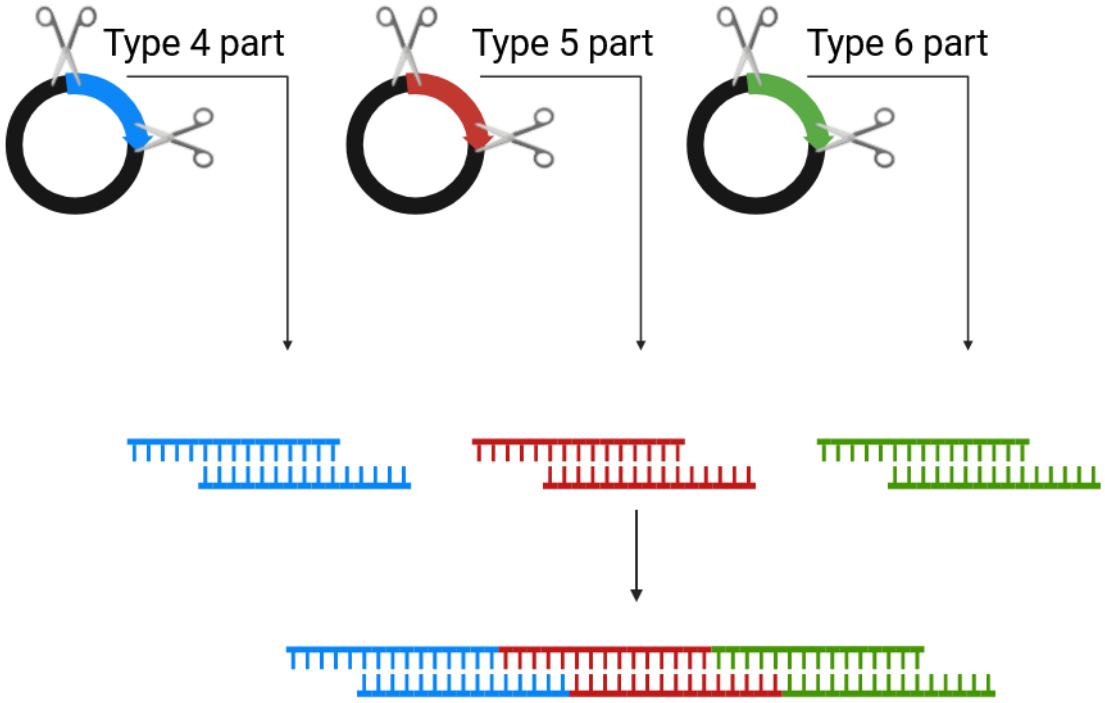

Figure 6: Illustration of how assembling consecutive MoClo parts works - using type 4 to 6 parts as an example.

acetaldehyde dehydrogenase (*ALD*) family, and is therefore closely related to *ALD5*. *ALD6* accounts for the major conversion of acetaldehyde to acetate [17], and its deletion is therefore of interest in improving *S. cerevisiae's* proliferation in acetic acid-rich environments. Figure 7 shows the metabolic pathway map for LX6 and visualizes how deletion of *ALD6* prevents the formation of acetate.

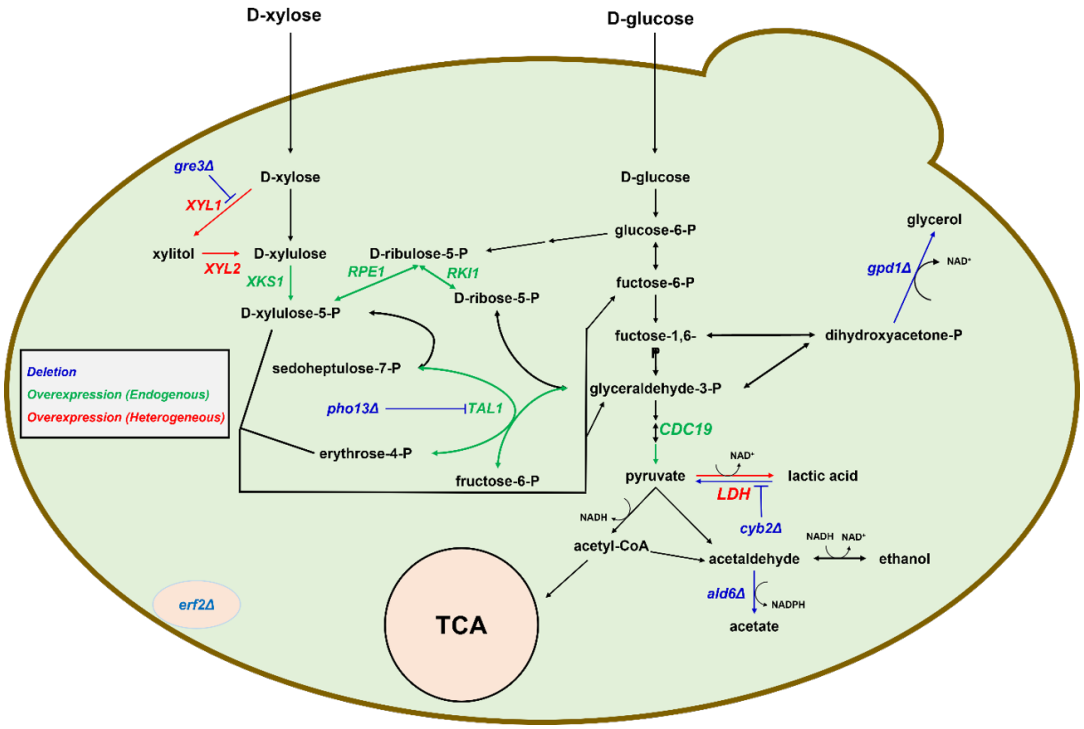

Figure 7: Metabolic pathway map for the *S. cerevisiae* strain, *LX6*. Image source: Choi et al., *Engineering of Saccharomyces cerevisiae for enhanced metabolic robustness and L-lactic acid production from lignocellulosic biomass* [36].

1.7 Aim

This master's thesis aimed to investigate the efficacy of the gRNA-landing pad strategy in *S. cerevisiae*, using the 'dispersed sgRNAs' and 'sgRNA-array' method - with the goal of improving the organism's acetate utilization.

Subgoals in this project are:

- Integrate the acetic acid biosensor in the genomic DNA of the LX6 strain and evaluate its performance.
- Design and validate Cas12 sgRNA-sequences for multiplexing
- Design and validate the gRNA-landing pads for multiplexing
- Transform segregant *S. cerevisiae* strain using Cas12, Cas12 sgRNA and gRNA-landing pads

2

Methods & Materials

2.1 *S. cerevisiae* strains and plasmids

The *S. cerevisiae* strains that were used in this project were the LX6 strain, as well as its segregants that were created from transformation of it. In Table 1 there is an overview of the different segregants, and how their genotype differs from the LX6 strain.

Table 1: *S. cerevisiae* strains used in this project.

***S. cerevisiae* strains**

Strain name	Genotype	Origin
LX6	ald6Δ::TEF2p-*CDC19*-CYC1t	Choi et al., paper **BoHyun2024**
LX7	LX6 ura3Δ::pMM4_14U	This study

Table 7 in appendix A provides an overview of the different plasmids used in this project, as well as their function and how they differs from their parent plasmid. Note that there are plasmids for use in *E. coli*, *S. cerevisiae*, as well as in both microorganisms.

2.2 *E. coli* media and culture conditions

E. coli was grown in liquid LB-media containing; 1 wt.% Tryptone, 1 wt.% NaCl, and 0.5 wt.% Yeast extract. Cultures were grown overnight in a 37°C shaking incubator. For culturing *E. coli* on agar plates the same conditions as for the liquid LB-media were used, but with the addition of 2 wt.% Agar-agar. These agar plates were also generally grown overnight at 37°C.

When there was a need to use antibiotic media conditions the appropriate antibiotic was added to the liquid LB-media, or the agar plate media before solidification. Antibiotics were taking from a stock concentration and diluted in said media to the working concentration in accordance with Table 2

Table 2: Antibiotics used for *E. coli* culturing and selection. Working concentrations are after dilution of the antibiotic in LB-media or agar plate media.

Antibiotic	Stock concentration	Working concentration
Ampicillin	100 mg/mL	100 μg/mL
Chloramphenicol	25 mg/mL	25 μg/mL
Kanamycin	50 mg/mL	50 μg/mL

Liquid LB-media was stored at room temperature, or in a dark 4°C refrigerator when containing antibiotics. LB-Agar plates were stored in a dark 4°C refrigerator. Overnight LB-media containing *E. coli* was never stored, it was always made fresh and immediately used. LB-agar plates containing *E. coli* were after overnight incubation stored in a dark 4°C refrigerator.

2.3 *S. cerevisiae* media and culture conditions

S. cerevisiae was grown in freshly made liquid YPD media containing: 2 wt.% Peptone, 1 wt.% Yeast Extract and 2 wt. % Glucose. *S. cerevisiae* was typically grown over 2-3 days at 30 °C. For culturing *S. cerevisiae* on agar plates the same conditions as for the liquid YPD-media were used, but with the addition of 2 wt. % Agar-agar. These agar plates were also generally grown over 2-3 days at 30 °C.

When there was a need to use antibiotic media conditions the appropriate antibiotic was added to the liquid YPD-media, or the agar plate media before solidification. Antibiotics were taking from a stock concentration and diluted to the working concentration in accordance with Table 3

Table 3: Antiobiotics used for *S. cerevisiae* culturing and selection.

Antibiotic	**Stock concentration**	**Working concentration**
Geneticin	50 mg/mL	200 μg/mL
Zeocin	100 mg/mL	200 μg/mL

To select for acetic acid biosensor integration in *URA3*, 5-FOA plates and uracil-deficient plates were used. The uracil-deficient plates were made using SC-URA powder and the 5-FOA plates by adding 5-FOA. Same culturing conditions as for regular YPD agar plates applied.

All strains of *S. cerevisiae* were preserved in a dark 4°C refrigerator when they were not used.

2.4 Molecular biology methods

During this project a plethora of molecular biology methods were used for various purposes. Below is an in-depth look at these methods and how they were applied.

2.4.1 PCR

During the course of this thesis three different types of PCR polymerases were used for amplification. They are listed below. 'Q5 High-Fidelity DNA Polymerase' PCR, simply referred to as 'Q5 PCR' was routinely used for amplification of genomic DNA from *S. cerevisiae* and plasmids when they were to be used for transformation or cloning, as Q5 PCR is highly accurate. Q5 PCR was performed in accordance with Protocol 1. Ligation temperatures were calculated using the NEBTm Calculator, and elongation time was found using SnapGene. Taq polymerase is generally considered to be low-fidelity when compared to the high-fidelity Q5. The Taq polymerase was mostly used for checking or verifying inserts or deletions. Taq polymerase PCR was performed in accordance with protocol 2. Ligation temperatures were calculated using the NEBTm Calculator, and elongation time was found using SnapGene. The Phire Hot start II DNA polymerse was used to perform 'PCR Colony' in this project. Colony PCR was used on colonies of either *E. coli* or *S. cerevisiae*. Colony PCR was performed in accordacne with protocol 3. Ligation temperatures were calculated using the Thermo fisher Tm calculator, and elongation time was found using SnapGene.

2.4.2 Gel electrophoresis

For routine verification of amplifications, assembly's and inserts, gel electrophoresis was performed. Gel electrophoresis was performed in accordance with protocol 4. To analyze the gel electrophoresis a

UV light-equipped gel imaging device was used.

2.4.3 Primer list

In table 8 in appendix A is a list of all primers used during this project, their sequence, as well as a description detailing how for what purpose they were used.

2.5 Restriction and ligation-based cloning of plasmids

Restriction of plasmids was performed in accordance with protocol 5, annealing of oligos was performed in accordance with protocol 6 and ligation-based cloning was performed in accordance with protocol 7. Specifics for how these protocols were used for the design of the Cas12 sgRNA plasmids are available in section 2.14.2, 'Cas12 sgRNA in-vitro.'

2.6 Transformation of *E. coli*

Electroportation tranformation of *E. coli* was performed in accordance with protocol 8. The highly competent 'TOP10 electrocompetent' *E. coli* were used for the transformations. After being plated on the appropriate media, the transformed *E. coli* were left to incubate at 37 °C.

2.7 Transformation of *S. cerevisiae*

Transformation of *S. cerevisiae* was performed using two variants of the Gietz method in accordance with protocol 9, and protcol 10. Protocol 9 was used for the integration of the biosensor, see section 2.11 and 2.12 for more details. Protocol 10 was used for the integration of the gRNA-landing pads, see section 2.13. After being plated on appropriate media the *S. cerevisiae* were left to incubate at 30 °C for 2-3 days.

2.8 Gibson assembly & the *ACS1*-construct

A construct consisting of *TEF1p*, *ACS1* and *PGK1t* was to be integrated into the genomic DNA of LX6, in the *HO* ORF. Amplification of the three parts making up the *ACS1*-construct was achieved through the use of three primer pair, all of which were tailed. For the PCR amplification of *TEF1p*, *ACS1*, and *PGK1t*, the respective annealing temperatures were used: 62 °C, 57 °C, and 59 °C. The three construct were then to be assembled through Gibson assembly, which relies on the aforementioned tails of the primers. One of the components of Gibson assembly which is crucial in this assembly is the T5 exonuclease - an enzyme which chews back on the 5' ends of DNA fragments, creating 3' overhangs [38]. The tails of the primers inside of the construct were designed to contain homology regions which when chewed back would be complimentary to each other. The primers on the outer ends of the construct instead contained arms homologous to the *HO* ORF. Gibson assembly was performed in accordance with protocol 11, using 100ng of each fragment.

2.9 Genetic DNA extraction of *S. cerevisiae*

To obtain genomic DNA from *S. cerevisiae* the 'Lithium-acetate' method was performed in accordance with protocol 12. During the later stages of the project genomic DNA was instead obtained using the 'NaOH' method as there sometimes were difficulties in amplifying DNA from the Lithium-acetate method. The DNA for the NaOH method was obtained in accordance with protocol 13.

2.10 The biolector

A biolector was used to grow *S. cerevisiae* in different acetic acid concentrations and with the different buffers, NaOH and KOH. Acetic acid concentrations were set between 0mM and 100mM, increasing

with 20mM increments between each step. The biolector was used to asses biomass over time, and fluorescence over time. Three replicates for each buffer and each concentration were used, resulting in a total of 96 samples being analyzed.

2.11 Integration of the initial biosensor

The YN2_1 HOi plasmid was created by restricting the *GFP* and its respective promoter and terminator gene from its parent plasmid, YN2_2_1_Cas9_gRNA, and introducing the oligos which form the gRNA targetting the HO promoter site. After transformation of *E. coli* those colonies which exhibited growth on ampicillin plates but no *GFP*-expression were restreaked and the YN2_1 IL50 plasmid was purified. Integration of the biosensor pMM4_14L in LX6 was performed in accordance with the GIETZ super protocol, protocol 9, using: 1000 ng restricted pMM4_14L biosensor for donor DNA and 500 ng of the YN2_1 HOi plasmid. Assessment of *GFP* expression was performed using fluorescence microscopy.

2.12 New strategy & Integration of the final biosensor

The biosensor pMM4_14L, which was originally intended to be integrated into the *HOp*, was exchanged for pMM4_14U. pMM4_14U is similar to pMM4_14L, but it contains no *GFP*. It has also had its *HOp* homology arms exchanged for arms which are homologous to the *URA3* ORF, instead of the *HOp*. This was done by performing a PCR on pMM4_14 using the two AP20 primers. These primers bind to *RET2p* and *SSA1t* of the plasmid respectively, and amplify the region between them which removes the *HOp* homology regions, geneticin resistance, and *URA3* from the plasmid. The primers also contain long tails which are homologous to *URA3*, facilitating integration of the biosensor in said loci. The changing of the integration target from the *HOp* to *URA3* was done for several reasons, first and foremost the previous attempts at integrating the biosensor into the *HOp* had been unsuccessful and it was decided to attempt a new angle at its integration. Secondly, by knocking out *URA3* this allows for future selection of landing pads which contain *URA3*, as well as counter-selection. Finally, it was decided that the landing pads would express *ymYPET*, a fluorescent protein which is similar to *GFP*. Removing *GFP* from the biosensor would therefore make it easier to measure *ymYPET*-expression.

The plasmid YN2_1_URA3 was created in the same way as YN2_1 HOi, but using oligos which target *URA3* instead of the *HOp*. Those *E. coli* colonies not expressing *GFP* after transformation were restreaked and the plasmid was purified. Integration of the biosensor pMM4_14L in the genome of LX6 was performed in accordance with the GIETZ super protocol, protocol 9, using: 1000 ng amplified pMM4_14U biosensor for donor DNA and 500 ng of the YN2_1_URA3 plasmid.

2.13 Design and assembly of the gRNA-landing pads

2.13.1 gRNA-landing pads in-silico

The gRNA-landing pads were designed to be integrated into the three different deletion-targets using SnapGene, and utilizing already existing parts from the MoClo library. Properties which were to be included in the gRNA-landing pads were: a fluorescent marker protein and subsequently a promoter and terminator expressing said protein, two ∼500bps homology arms flanking each deletion-target, and a *URA3* selection marker.

From the MoClo-YTK plasmid library a suitable promoter, terminator, ConE type connector, and *URA3* selectable marker were chosen. The fluorescent protein *ymYPET*, available in a plasmid previously developed by Luca Torello Pinale and Lisbeth Olsson[39], was chosen as the expression-target for the gRNA-landing pads. These aforementioned parts may when restricted from their respective plasmid together form a 'promoter-*ymYPET*-terminator-connector-*URA3*'-construct - a gRNA-landing

pad. To integrate the gRNA-landing pad into *S. cerevisiae* it needs to be flanked by regions homologous to the gene where it is to be integrated. This was done be designing primers which bind to the top and bottom strand, both upstream and downstream from the deletion-target. These primer pairs were designed with custom tails to create BsaI recognition sites on the outmost end of each homology arm so that restriction using BsaI also removes said recognition site. The sticky ends created by using BsaI is on one end of the upstream homology arm complimentary to the promoter part, and on one end of the downstream homology arm complimentary to the *URA3* part. The remaining sticky end on both the upstream and downstream homology arm were made to be complimentary to a final MoClo-YTK backbone part. This backbone plasmid was a *RFP*-dropout casette, and is also the only plasmid to contain an ampicillin resistance marker.

Using the restriction enzyme BsaI, all eight parts involved in creating each gRNA-landing pad restricted from their backboen and then ligated into a plasmid in-silico. Figure 8 illustrates how the procedure was done in SnapGene.

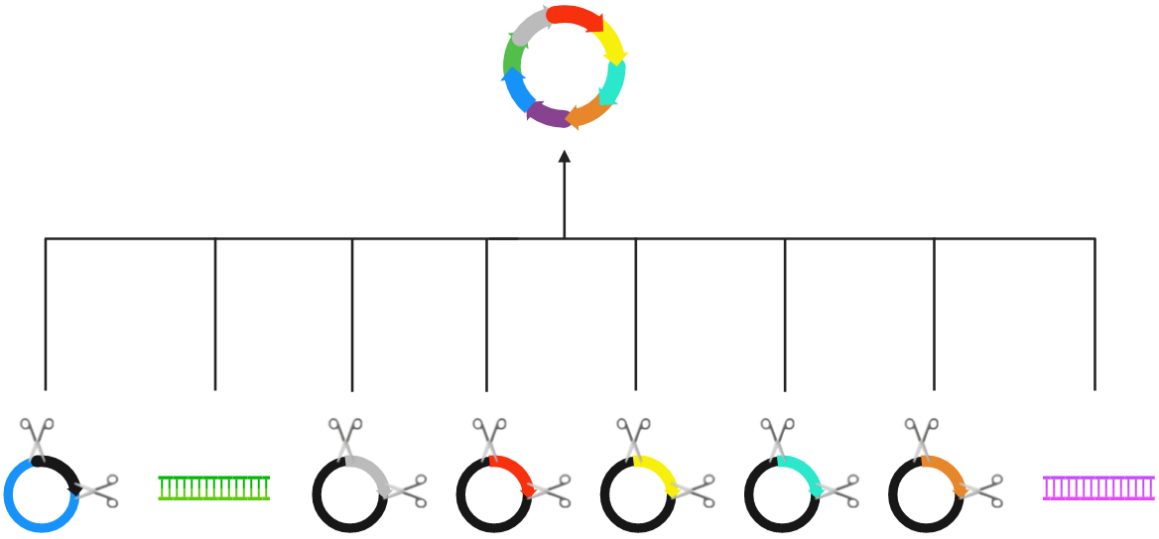

Figure 8: Illustration of how the eight parts making up each gRNA-landing pad were restricted and cloned into the backbone cassette.

2.13.2 gRNA-landing pads in-vitro

The plasmids were delivered in *E. coli* in LB agar plates. With the exception of LT04_4_ymYPET which was delivered in a liquid culture. The plasmids which were on the LB agar plates were inoculated to be in overnight liquid cultures as well. The amplified homology arms and plasmids in the liquid cultures were purified and had their concentration measured, see table 4. The resulting mixture was placed in 4 C°until assembly. To assemble the different parts into a the backbone, the Golden Gate Assembly protocol was used, see protocol 14. 75 ng of each plasmid and amplicon was used, and 30 restriction/annealing cycles were run before a final heat-inactivation step.

Electroporation transformation of *E. coli* was performed using the assembled gRNA-landing pads, and cells were streaked onto plates LB plates containing ampicillin and left to incubate overnight. In the morning colonies which exhibited growth and did not express *RFP* were replated onto new LB-ampicillin plates and left to incubate overnight again.

Table 4: Measured concentration used NanoDrop, for the six plasmids to be used in the golden gate assembly.

Plasmid or Amplicon	Concentration
pYTK083	350 ng/µl
pYTK017	115 ng/µl
LT0_4_ymYPET	187 ng/µl
pYTK052	94 ng/µl
pYTK067	150 ng/µl
pYTK074	150 ng/µl
GOR1LeftArm	54 ng/µl
GOR1RightArm	20 ng/µl
ALD5LeftArm	42 ng/µl
ALD5RightArm	33 ng/µl
HXK2LeftArm	139 ng/µl
HXK2RightArm	140 ng/µl

2.14 Design and assembly of the Cas12 sgRNA

2.14.1 Cas12 sgRNA in-silico

The first step in the design process of the Cas12 sgRNA was the to find suitable protospacers and PAM sites in the deletion-targets. To do this the Centre for Organismal studies' 'CCTop - CRISPR/Cas9 target online predictor' and Benchling were used. Only PAM sequences near the middle of each deletion target were investigated. Those sequences with the highest efficacy and lowest off-target score were selected for each, these are seen in table 5.

Table 5: Protospacers, PAM sites, and loci for the three deletion-targets.

Gene	Protospacer	PAM site	Chromosome: position
GOR1	AGAGAGATTGAAGCCGTTTG	TTTA	XIV: 121 614 - 121 634
HXK2	CGGCTGGACTCAAACCTCAC	TTTA	VII: 25 250 - 25 270
ALD5	GTGCGCGCGGTGACGTCGCT	TTTG	V: 304 371 - 304 391

The crRNA_Cpf1_backbone plasmid was ordered from GenScript and had been designed as a *GFP*-dropout cassette - having BsmBI restriction sites flanking the fluorescent protein's promoter and terminator. Upon restriction with BsmBI the crRNA_Cpf1_backbone plasmid has the 3' overhang 'GGGA' and the 5'overhang 'AACG'. The sgRNA was therefore designed to have overhangs complimentary to those of the backbone plasmid. The sgRNA for was also designed to have a direct repeat (DR) region recognised by Cas12a/LbCpf1 before the protospacer sequence. In figure 9 the oligos making up the *GOR1*-targeting sgRNA have been annealed in-silico, with overhangs complimentary to 'GGGA' and 'AACG'.

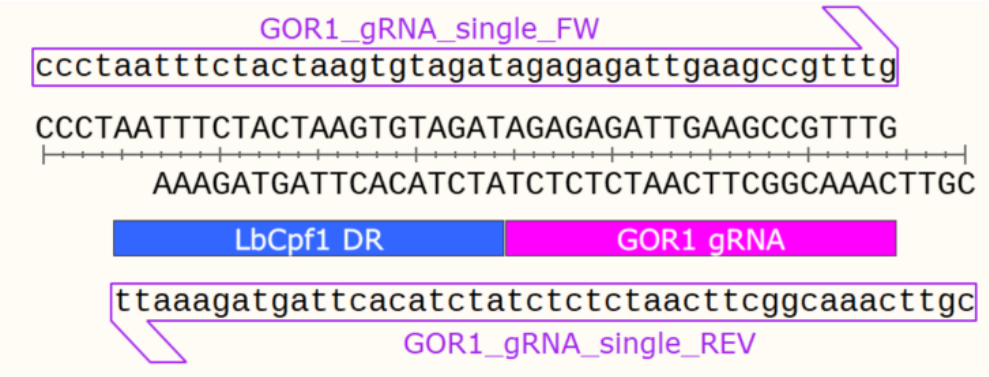

Figure 9: The two oligos making up the *GOR1* sgRNA annealed in-silico, in SnapGene. The annealed oligos contain a direct repeat region, the protospacer for targetting *GOR1*, and overhangs on each side.

As for the sgRNA-array a similar approach was used, with the major difference being the overhangs complimentary to those of the backbone plasmid were reserved for the 5' end of the first sgRNA in the array, and the 3' end for the last. For the sgRNA-array the overhangs between the different sgRNAs were designed uniquely, so that the array could only be assembled in the order: *HXK2, ALD5, GOR1*. In-silico assembly of the plasmid crRNA_Cpf1_array was performed successfully by annealing the sgRNA array into the crRNA_Cpf1_backbone plasmid using SnapGene. Figure 10 illustrates how the assembly was performed.

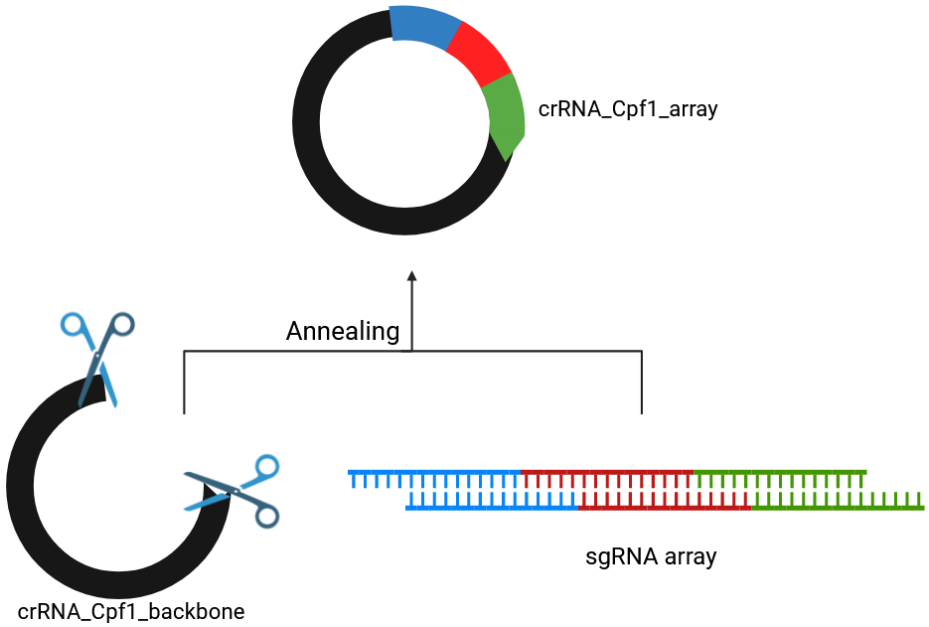

Figure 10: Annealing of sgRNA array containing 'CCCT-overhang'-*HXK2-ALD5-GOR1*-'TTGC-overhang' and the BsmBI-restricted crRNA_Cpf1_backbone plasmid - creating the cRNA_Cpf1_array plasmid.

2.14.2 Cas12 sgRNA in-vitro

For creation of the single-target sgRNAs 1 ng of the plasmid crRNA_Cpf1_backbone was restricted using BsmBI restriction enzymes, in accordance with protocol 5. After the restriction and heat inactivation it was stored at 4 °C. The single-target sgRNA oligos were annealed and stored at 4 °C. The restricted crRNA_Cpf1_backbone plasmid was placed in three separate PCR tubes, and a unique set of single-target annealed sgRNA oligos were added to each tube. The ligation was performed and the resulting plasmid were stored at 4 °C until transformation. As for the sgRNA-array a similar approach was followed. In this case however, each oligo was first phosphorylated using a T4 polynucleotide kinase, and then annealed together in pairs. This was followed by annealing the three pairs together with 50 ng of the cut crRNA_Cpf1_backbone plasmid. Both the annealing of the single-target sgRNA and the sgRNA-array was performed according to protocol 6, and the ligation-based cloning according to protocol 7.

The transformation was performed using electroporation transformation of TOP10 electrocompetent *E. coli*. The cells were plated on LB-ampicillin plates and left to incubate overnight. In the morning colonies which did not express *GFP* and exhibited growth on the LB-ampicillin were restreaked and left to incubate overnight.

2.15 Design of the sgRNA-landing pad integration strategy.

Originally a combination of sgRNA plasmid and linearised sgRNA plasmid, sgRNA-landing pad plasmid and linearised gRNA-landing pad, as well as Cas12 in plasmid and Cas12 amplified from plasmid were supposed to be used to the transformation. However, restriction of the sgRNA plasmid and the gRNA-landing pad proved difficult resulting in the final transformation plan being altered. It was then decided that six different permutations of Cas12, sgRNA and gRNA-landing pad were to be used for the introduction of the gRNA-landing pad in LX7, these are seen in table 6.

Table 6: The six different permutations of Cas12 / Cpf1, sgRNA, and gRNA-landing pad that were used for the transformation of LX7.

No.	**Cas12 / Cpf1**	**GOR1 sgRNA**	**gRNA-landing pad**
1	Amplified from plasmid (450ng)	In plasmid (500ng)	In plasmid (1000ng)
2	In plasmid (500ng)	In plasmid (500ng)	In plasmid (1000ng)
3	In plasmid (500ng)	Backbone plasmid used instead (500ng)	In plasmid (1000ng)
4	In plasmid (500ng)	Backbone plasmid used instead (500ng)	None
5	In plasmid (500ng)	In plasmid (500ng)	None
6	Amplified from plasmid (450ng)	In plasmid (500ng)	None

After transformation each permutation was plated out on two plates; one SC-URA + geneticin plate, and one SC-URA plate. The cultures were left to incubate for 3 days before they were taken out to room temperature.

3

Results

3.1 Biosensor integration in *S. cerevisiae*

3.1.1 Initial biosensor - pMM4_14L

The biosensor pMM4_14L was cut out from its backbone using NotI and verified using gelelectrophoresis. In-silico restriction indicates that backbone should be ∼9600bps and the restricted biosensor ∼1800bps. Figure 11 indicates the the restriction was successful.

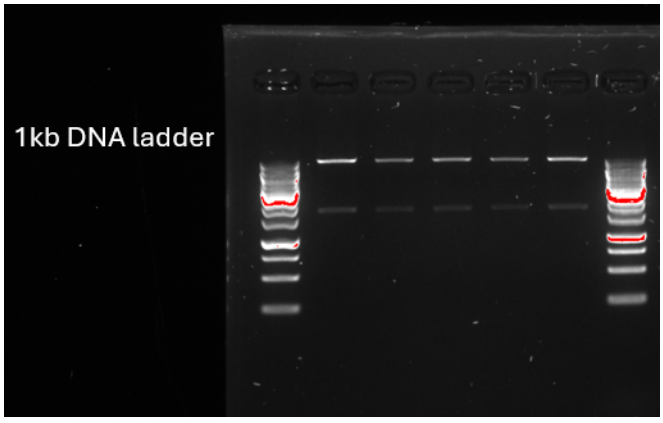

Figure 11: 5 replicates of the restricted pMM14_4L, with 1kb DNA ladders on each side.

In the first attempt at the LX6 transformation only geneticin was used as a selection marker. None of the transformants appeared to exhibit *GFP*-expression, indicating that the integration of the biosesor was unsuccessful. One of the transformations done without donor DNA — that is, without a biosensor — had many colonies. This transformant was meant to act as a negative control, as it was expected to cut the genomic DNA without providing any donor DNA for HDR. This indicated the geneticin resistance from the YN2_1 HOi was expressed, without the genomic DNA being cut. It was then decided to utilize the Zeocin resistance marker in the pMM14_4L biosensor to improve the control.

In the second attempt at transforming LX6 using the pMM14_4L biosensor it was initially thought that the transformation was successful, as many colonies appeared to express *GFP* on the Geneticin + Zeocin media. When compared to the positive control however, it became clear that what was thought to be *GFP*-expression was more likely *S. cerevisiae's* autofluorescence.

3.1.2 Final biosensor - pMM4_14U

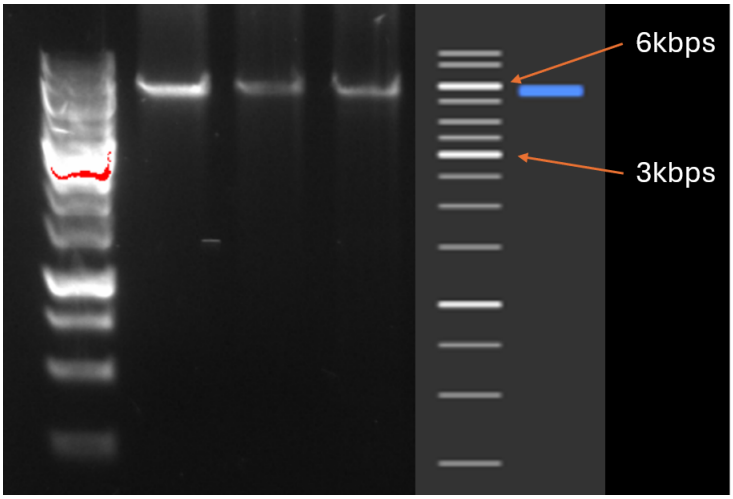

Figure 12: Amplification of the biosensor pMM4_14, using the AP20 primer pair. To the right is comparison to in-silico amplification.

After transformation of the LX6 strain using YN2_1_URA3 and the biosensor pMM14_4U there were no colonies on the SC 5-FOA agar plate. There were however some colonies on the YPD geneticin plate. These were restreaked on SC media with and without uracil. No colonies grew on the media without uracil. Those colonies exhibiting growth on the SC media had their DNA amplified using Colony PCR and the primer pairs: AP1_RET1p_RV + AP37_URA3_OUTSIDE_FW, and AP37_URA3_OUTSIDE_REV + AP38_SSA1t_REV. When comparing the bands from each of the colonies with those obtained using in-silico amplification in SnapGene, see figure 13, it appears as if the integration is successful for three of the colonies. Thus the strain LX7 was successfully created from its parental strain LX6 by introducing the biosensor pMM14_4U into the *URA3* loci.

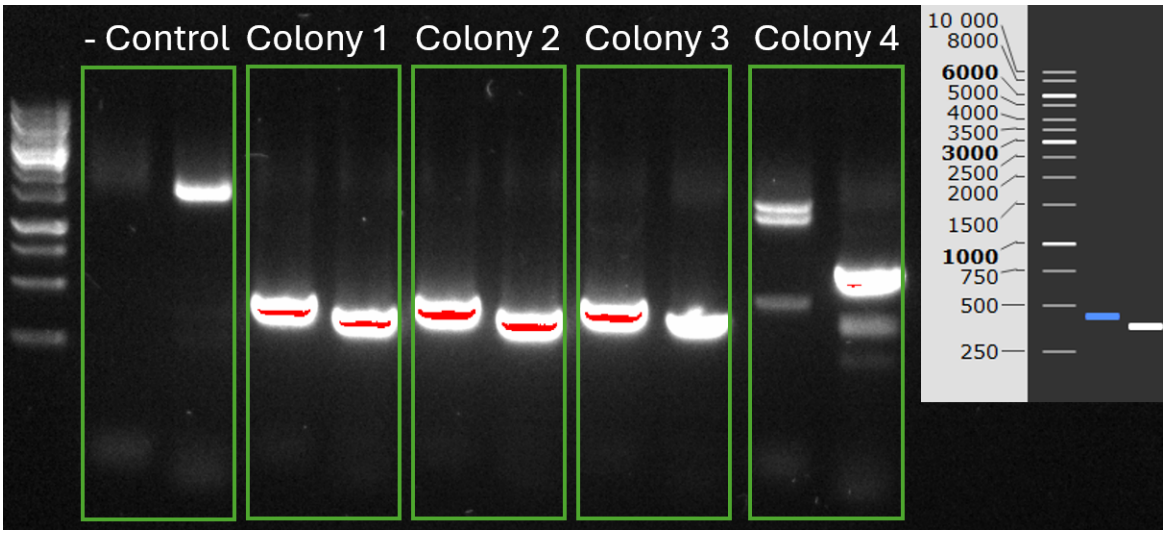

Figure 13: Amplification of 4 colonies which survived on YPD geneticin plates and exhibited growth on 5-FOA media. Negative control is LX6. For each colony the leftmost band is the AP1_RET1p_RV + AP37_URA3_OUTSIDE_FW primer pair, and the righmost band is the AP37_URA3_OUTSIDE_REV + AP38_SSA1t_REV primer pair. To the right is comparison to in-silico agarose gel.

3.2 *ACS1*-construct assembly results

The three different parts making up the *ACS1*-construct were after amplification put on gel, see figure 14. There are visibly bands for all three genes, even though bands for *TEF1p* were very faint, this should be enough for Gibson assembly.

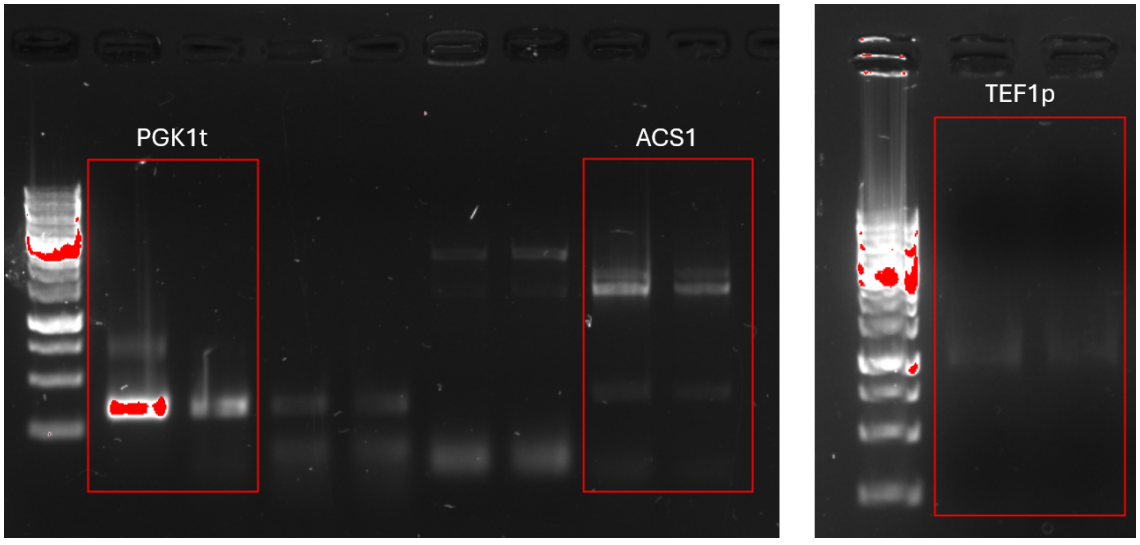

Figure 14: Amplification of the three parts making up the *ACS1*-construct.

The Gibson assembly was then performed, annealing the three different parts into one construct of

length ∼3500bps. Subsequent gel electrophoresis of the construct was ambiguous, and contained many smeared lines, see figure 15. Nonetheless, a purification was performed to separate what was believed to be the *ACS1*-construct from the incorrect bands. PCR was performed on the gel-purified DNA, the following gel electrophoresis came back blank. As the introduction of the *ACS1*-construct into the HO ORF had not yet reached the transformation stage it was decided to abandon this approach, and instead possibly have *ACS1* act as another over-expression target to be integrated into the landing pads in the future.

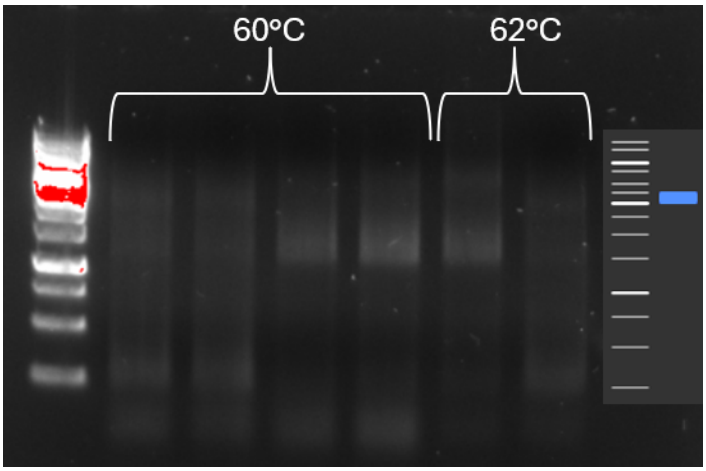

Figure 15: Gibson assembly performed at two different temperatures. Correct assembly in-silico is seen to the right, at ∼3500bps. Reference DNA ladder is 1kb.

3.3 Transformation of *E. coli* using the Cas12 sgRNA.

Figure 16 shows the results of the first restreaking, where only the colonies with the *GOR1* sgRNA exhibits growth on LB-ampicillin and do not express *GFP*. Transformation and restreaking was repeated for the two other sgRNAs, as well as for the sgRNA-array until there had been colonies isolated from each assembly which exhibited growth on LB-ampicillin but did not express *GFP*.

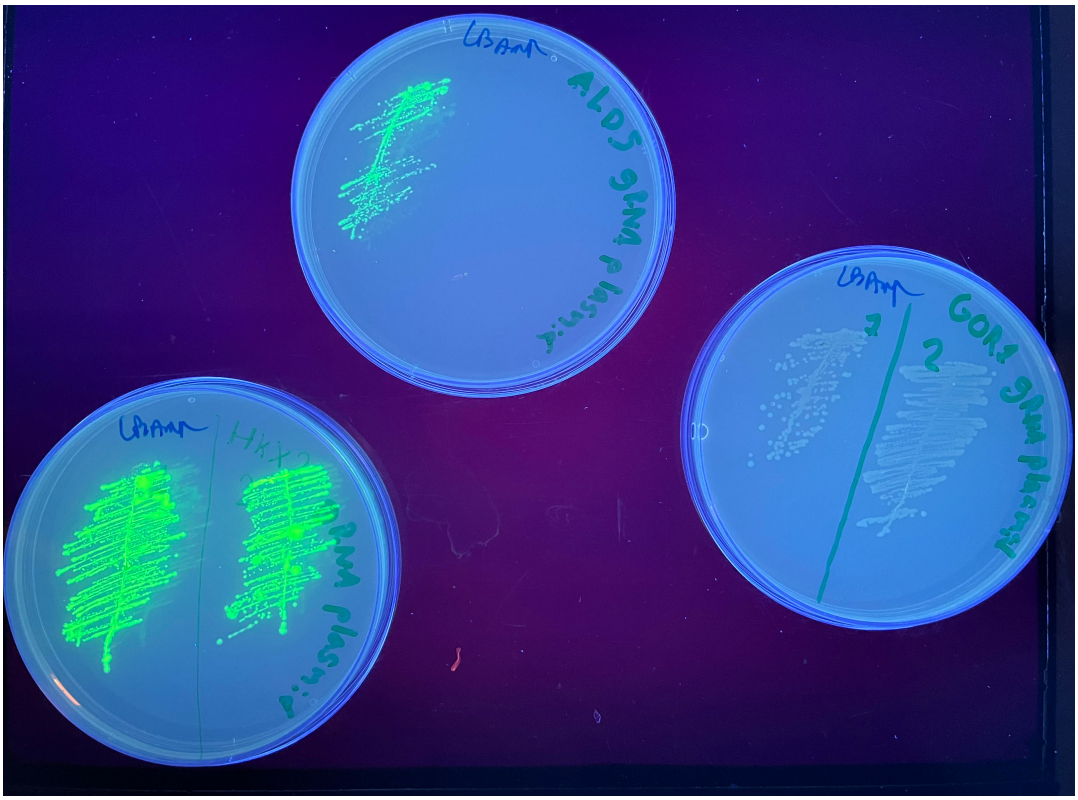

Figure 16: From left to right, initial assembly attempt for the three single-target Cas12 sgRNAs after transformation of *E. coli* : *HXK2*, *ALD5*, and *GOR1*.

All four Cas12 sgRNA transformants exhibiting growth on LB-ampicillin plates while not expressing *GFP*: crRNA_Cpf1_GOR1, crRNA_Cpf1_HXK2, crRNA_Cpf1_ALD5, and crRNA_Cpf1_array, were sent for sequencing using the AP41 primer pair. Sequencing revealed that all plasmids had been successfully assembled.

3.4 Transformation of *E. coli* using the gRNA-landing pads

In figure 17 the results from the restreaking of *E. coli* transofrmed with the *GOR1* gRNA-landing pad can be seen. Only one out of 10 colonies which at first appeared to not express *RFP* turned out to actually not express the fluorescent protein. *RFP* was quite difficult to see immediately after overnight incubation, it usually took a couple of additional hours in room temperature until the *RFP* became clearly visible.

The *E. coli* transformed with the *GOR1* gRNA-landing pad which exhibited growth on LB-ampicillin plates and did not express *RFP* had their plasmids purified and sent for sequencing, using the primers AP48 and AP51. Initial sequencing revealed that the *GOR1* gRNA-landing pad was successfully assembled.

The *E. coli* transformed with the *HXK2* and *ALD5* gRNA-landing pad were plated on a different batch of LB-ampicillin plates than those used for the *GOR1* gRNA-landing pad. On these plates there were a lot of satellite colonies. Still, the plasmids were purified and sent for sequencing. When the sequencing revealed that the assembly of the *HXK2* and *ALD5* gRNA-landing were unsuccessful a new

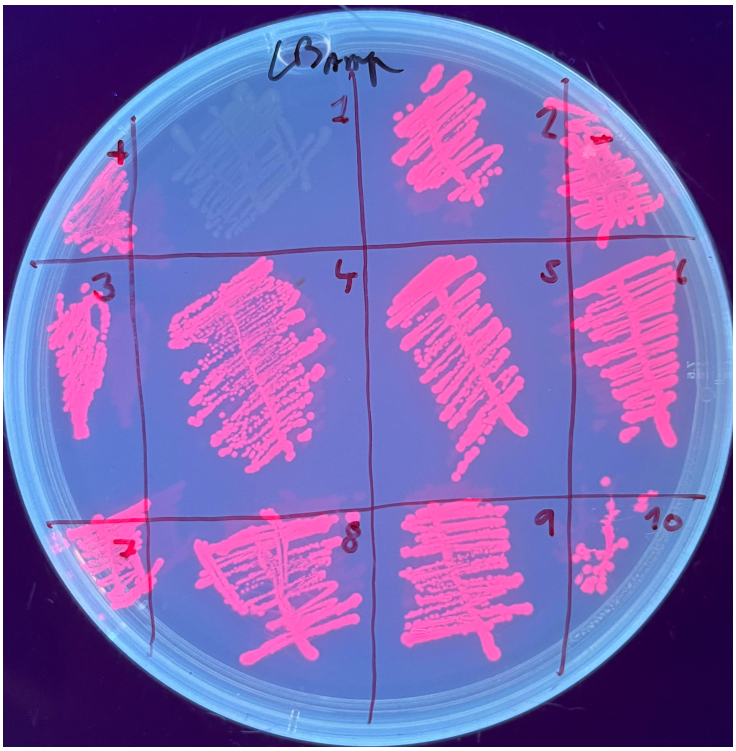

Figure 17: Replated *E. coli* which have been transformed using the *GOR1* gRNA-landing pad from the golden gate assembly. Colony 1 is the only one not expressing *RFP* but still exhibiting growth on LB-ampicillin plates, indicating that the gRNA-landing pad has been successfully assembled.

set of LB-ampicillin plates were prepared, and the transformation was repeated - this time no satellite colonies appeared for the *E. coli* transformed with the *ALD5* gRNA-landing pad. These colonies not expressing *RFP* but still exhibiting growth on LB-ampicillin media had their plasmid purified and sequenced, with the sequencing indicating the succesfull assembly of the *ALD5* gRNA-landing pad. As for the *HXK2* gRNA-landing pad no *E. coli* exhibited growth on LB-ampicillin while not expressing *RFP*.

Before the *E. coli* containing the *ALD5* gRNA-landing pad which exhibited growth on LB-ampicillin plates while not expressing *RFP* was sent for sequencing it was compared to the successfully assembled *GOR1* gRNA-landing pad using primers. The plasmids were purified and amplified using the primer pairs: AP48 + AP51, AP44 + AP48, and AP43 + AP48. The bands created from amplification of the supposedly assembled *ALD5* gRNA-landing pad were identical to those that were amplified from the *GOR1*-gRNA landing pad, indicating that the *ALD5* gRNA-landing pad had been successfully assembled, see figure 18.

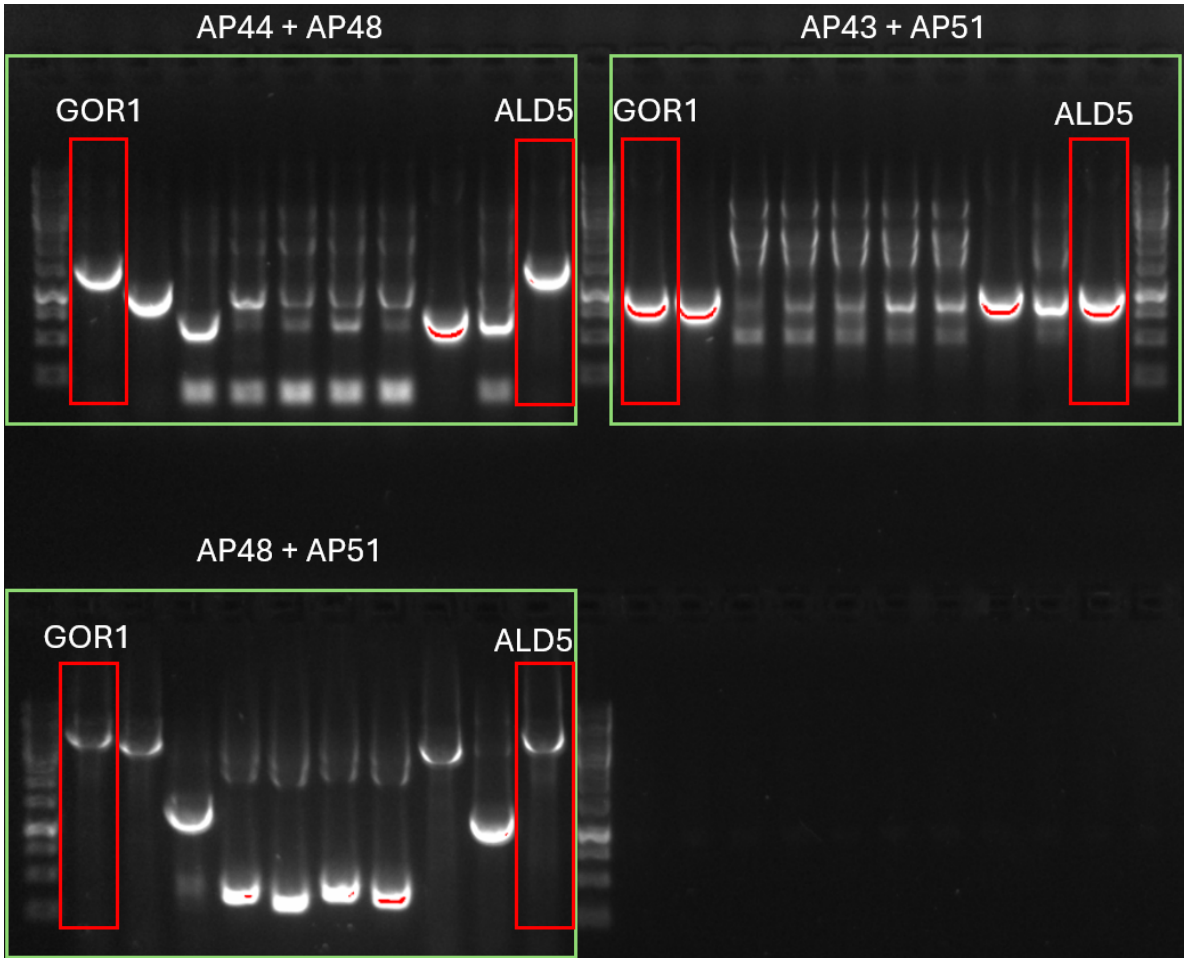

Figure 18: Amplification of the previously sequenced correct *GOR1* gRNA-landing pad, compared to *ALD5* gRNA-landing pad using various primers.

3.5 Introducing the gRNA-landing pads in LX7

Note that the *ALD5* gRNA-landing pad is not involved in this section due to its assembly being correct during later stages of the project. The gRNA-landing pad here refers to the *GOR1* gRNA-landing pad.

For the transformation an original 8 different permutations of the sgRNA, the gRNA-landing pad and the Cas12 were supposed to be used. This required the gRNA-landing pad and the sgRNA to be cut from their respective backbone. Upon gel electrophoresis of the newly restricted gRNA-landing pad and sgRNA it was however revealed that this restriction had not been successful. The sgRNA plasmid which had been cut using PstI and EcoRI did have two bands as it should, but these bands did not match with the in-silico bands with lengths 3787bps and 1273bps, see figure 19. The gRNA-landing pad showed more than two bands, which should not be possible as it only has two restriction sites for the enzyme BsaI, which was used to restrict it, see figure 20. These two bands were in-silico observed to be 1870bps and 3929bps.

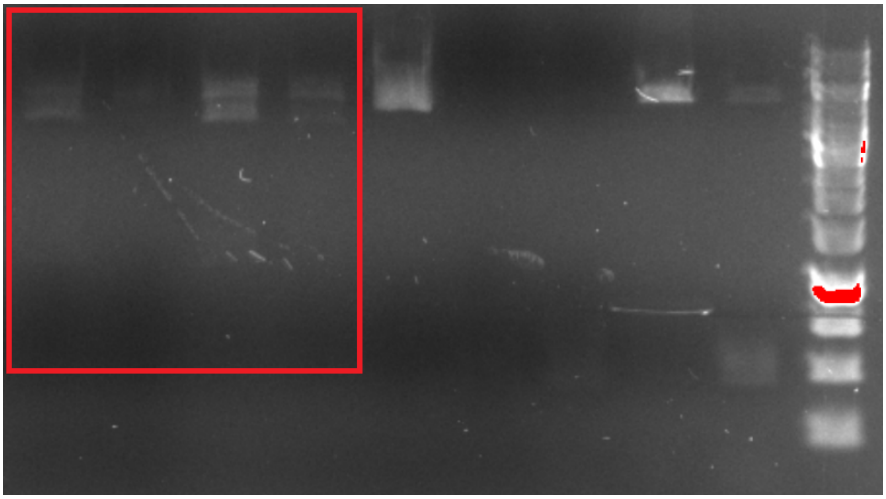

Figure 19: Highlighted in red is the sgRNA plasmid which has been cut by PstI and EcoRI. To the far right is a 1kb DNA ladder which indicates that the two bands observed for the restricted sgRNA plasmid do not appear to be of the correct lengths: 3787bps and 1273bps.

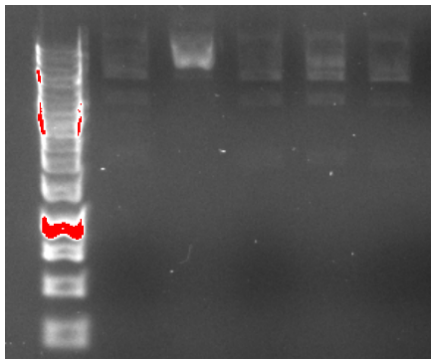

Figure 20: *GOR1* gRNA-landing pads restricted by BsaI with 1kb DNA ladder for reference to the left. More than two bands are clearly visible for all wells, with the exception of the second well were it appears as if the plasmid was not restricted. The expected lengths of the two bands were: 1870bps and 3929bps.

Transformation of *S. cerevisiae* LX7 was performed using the six permutations seen in table 6. Upon analysing the plates it was however revealed that no *S. cerevisiae* appeared to have survived - indicating that the transformation, the introduction of the *GOR1* gRNA-landing pad, had not been successful.

3.6 Analysis of the LX7 strain

The LX7 strain was grown in the 96-well plate in a biolector with varying acetic acid conditions. The mCherry-expression and biomass of the LX7 strain was then compared to its parental strain, see figure 21 and figure 22. Overall a trend of increasing mCherry-expression over biomass can be observed from 0mM to 40-60mM acetate. LX7 appears to grow slightly slower than its parental strain.

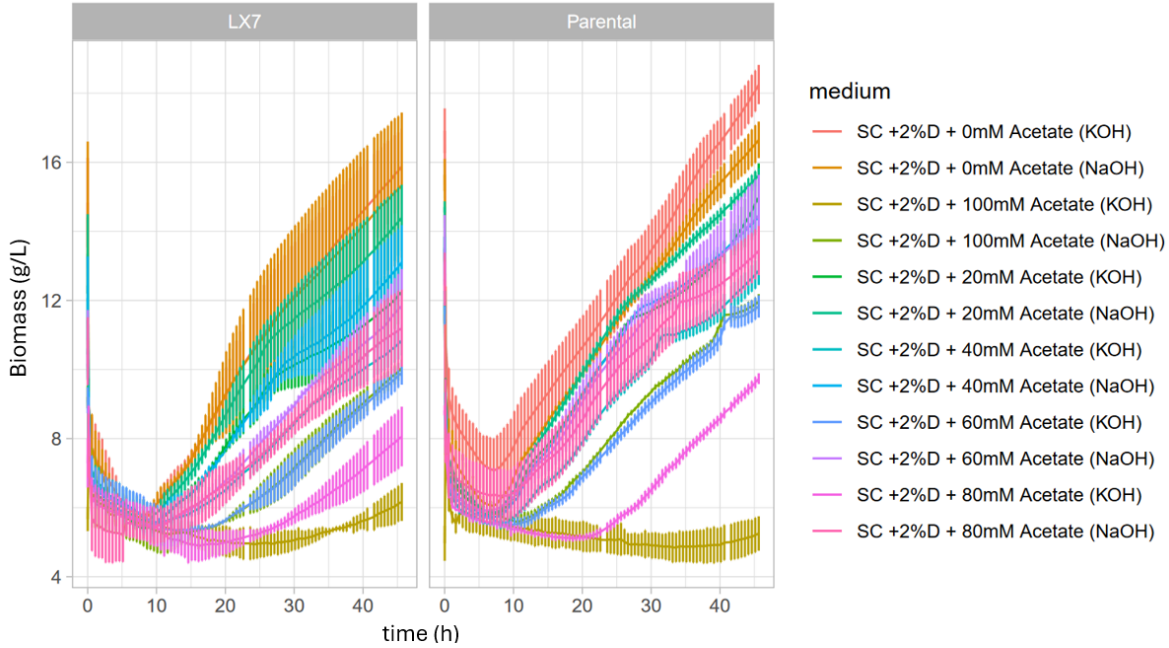

Figure 21: Biomass (g/L) over time (h) for different concentration of acetate and buffers. Comparison of LX7 versus parental strain. Width of each line indicates one standard deviation.

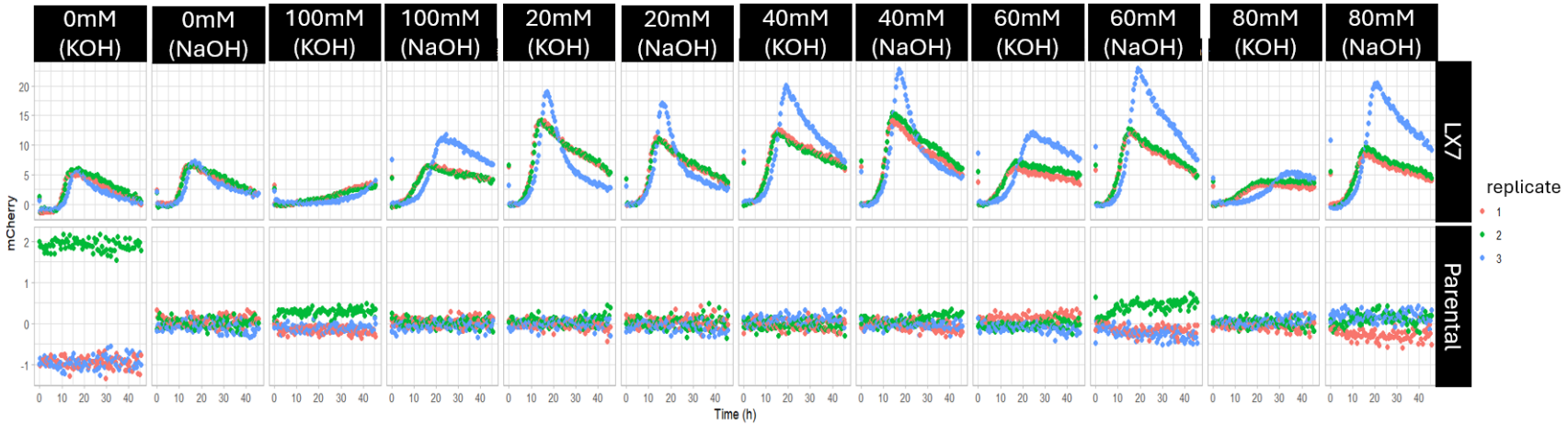

Figure 22: The image displays the comparison of mCherry fold of induction divided by biomass during 40 hours in the biolector for various concentrations, buffers, and strains using three replicates.

4

Discussion

In this chapter the results, as well as their implications, will be discussed with the current scientific paradigm in mind.

4.1 *ACS1* and Gibson assembly

The Gibson assembly of the *ACS1*-construct was not successful. Had the amplification of TEF1p, *ACS1*, and PGK1t been achieved earlier than it was this would have provided more time to trouble-shoot the Gibson assembly, as for now, one is left to hypothesize. T5 exonuclease, the enzyme responsible for degrading double-stranded DNA in a 5' to 3' direction, plays an essential role in the Gibson assembly method - creating single-stranded DNA out of the complimentary tails located on each part of the assembly. There is however evidence that the T5 exonuclease may also exhibit endonuclease activity - that is, degrading the 3' ends of the single-stranded DNA that it creates by its own exonuclease activity [40]. In a study by Rabe and Cepko they have conducted comparisons between the efficiency and accuracy of three different formulations for the Gibson assembly; the Original assembly by Gibson et al., the NEB HiFi which was used in this project, and the 'Enhanced' formulation which they described in their paper [38]. They described how by adding a single-stranded DNA-binding protein this provides protection to the single-stranded DNA which is created by T5 exonuclease activity - protecting it from endonuclease activity. While they do not directly quantify the correctly assembled inserts for each of the formulations, they do so indirectly by comparing the percentage of correctly transformed *E. coli* expressing the phenotype of their assembly - this provides an indication as to what formulation provides the most accurate assembly. For a 2-insert assemble there is no notable difference between the formulations. For a 6-insert however, their 'Enhanced' formulation provides an 80% correct assemble rate, compared to the NEB HiFi's 45% and the original's 20%. It is difficult to tell how much of a difference using the enhanced formulation would have made for the Gibson assembly. In general, Gibson assembly is quite efficient and a single successfully assembled construct should be enough for subsequent PCR. Had there been more time, this enhanced approach could have been attempted, as well as general trouble-shooting by attempting gradient PCRs and tweaking of ligation and extensions times.

4.2 Discussing the transformation of LX7

The transformation of LX7 using the *GOR1* gRNA-landing pad gave no live colonies. This provides quite the conundrum as it now becomes impossible to tell whether is was the Cas12, the *GOR1* sgRNA or the *GOR1* gRNA-landing pad that does not work. Of course, there is always the possibility there were errors in the experimental procedure led to this outcome.

The Cas12 plasmid used, has previously been demonstrated to work very well, almost having a 100% editing efficiency [41]. It should however not be ruled out as a possible source of error. In the study where this extremely high editing efficiency was measured the yeast had already been transformed to express Cas12 before it was transformed with the sgRNA and donor DNA. Which differs from the approach taken in this project, where transformation of the Cas12 plasmid occurred at the same time as with donor DNA and sgRNA. This is in general not a problem, such called 'co-transformations,' where just a single transformation is needed to insert sgRNA, Cas-systems, and donor have demonstrated very high editing efficiencies - even in multiplexing systems [42]. In this thesis however, a Cas12-system

was used. There might be differences in how the still relatively new Cas12-system operates when compared to the more conventional Cas9-system. In another Paper, by Zhang, L., Zuris, J.A., and, Viswanathan, R. et al., the authors describe the AsCas12a ribonucleoprotein as exhibiting "relatively poor editing efficiency" - with the LbCas12a ribonucleoprotein, which was used in this thesis, only being marginally more efficient [43]. Another noteworthy observation is that in the latter paper the authors also perform an initial transformation using only the Cas12 and no donor DNA. While it is not possible to tell whether a similar approach would have made a difference in this project, using said method could present an alternative should future transformations remain difficult. The Cas12 plasmid used in this thesis already contains a Kanamycin resistance marker, enabling easy selection if this would be attempted.

Another aspect to consider is that the *GOR1* gRNA-landing pad donor DNA was not linearized, as originally intended. This could have various detrimental effects on the transformation. If the gRNA-landing pad plasmid is successfully integrated in the yeast its expression of said landing pad would be unpredictable. High expressions of double-stranded DNA, especially long sequences such as the gRNA-landing pad, have been found to be toxic [44] [45]. With that being said, having a transient donor DNA plasmid is generally a viable strategy that has been employed before. In an article by Oh, et al., which albeit concerns T Cells, using linear double-stranded DNA and donor DNA in a plasmid is compared [46]. The findings in this paper echo the same sentiment - higher concentrations of double-stranded DNA donor drastically reduce cell viability, while somewhat improving transformation efficiency.

The homology arms were designed to be homologous the region outside of the gene where they were to be integrated. This was done to ensure that upon integration of the landing pad there would be no undesired effect from half of the genes being expressed. It is possible that the distance between the Cas12-induced double-strand break and the homology arms is too great. In a paper by Paquet et al., the percentage of successful transformations went down from 99.7% to 23.5% as the 'cut-to-mutation distance' went from 2bps to 23bps in human induced pluripotent stem cells. Extrapolating this principle to apply to *S. cerevisiae*, even the slightest, would suggest that the >1000bps cut-to-mutation distance of the gRNA-landing pads in this thesis would have a negative effect on the percentage of successful transformation. Furthermore, studies have found that as little as 15bps of homology is sufficient for knock-in of smaller constructs - given that the homology arms directly flank the ribonuclease-induced double-strand break [47]. If half a gene being expressed remains a concern, an alternate method to address this could be to integrate the gRNA-landing pad further upstream in its target gene in such a manner that the rest of the gene is frameshift mutated.

4.3 Prospects for the gRNA-landing pad assembly

The original YTK MoClo kit has homology arms that can be used to integrate a gRNA-landing pad in a select few loci: *URA3, LEU2* and the HO ORF. While this can be useful, this project aimed to introduce gRNA-landing pads into other loci, loci for which there were no pre-existing plasmids with homology arms available. The successfully assembled *ALD5* and *GOR1* gRNA-landing pad demonstrates the possibility of creating gRNA-landing pads for integration anywhere in the genome of *S. cerevisiae*, using the already existing YTK MoClo kit and four tailed primers. The primers can be moved anywhere along the genome to create homology arms as long as their tails remain the same.

4.4 Analysis of LX7

In a paper by Mormino, M., Lenitz, I., Siewers, V. et al., the biosensor pMM4_14L was integrated in *S. cerevisiae*, and the mCherry-expression was measured. This revealed a trend where the expression of the mCherry increased drastically as the concentration acetic acid increased from 0mM to 20mM, only to much more slowly increase as the concentration acetic acid approached 50mM, where the increase in mCherry-expression appears to stop [34]. In this thesis the results are very similar, with mCherry

expression reaching its peak at around 60mM acetic acid. While there is some deviation within the replicates - most notable replicate three seems to induce more mCherry expression - it appears as if the pMM4_14U biosensor works as similarly to how pMM4_14L did in the aforementioned paper - as intended.

Concerning the growth of the LX7 strain, it seems to be slightly reduced when compared to the parental LX6 strain. As the strains are grown in media containing *URA3*, the knock-out of said gene in LX7 should not make a difference. There is however evidence indicating that *S. cerevisiae's* ability to absorb certain nutrients is impaired during acetic acid-induced stress. In a paper by Ding et al., *S. cerevisiae* deficient of *URA3* was grown in YNB + 2% glucose media containing no acetic acid, and 80mM acetic acid. The results showed that uracil uptake was halved in the cells without *URA3* [48]. The authors performed further experiments where they uncovered that in the aforementioned conditions, the concentration of ATP in *S. cerevisiae* was approximately four times lower in the null-mutant cells compared to the wild-type. It would not be beyond reason to argue that this drastic change in ATP could potentially play a role in the slightly reduced biomass production observed by the *URA3*-knockout LX7 when compared to LX6.

5

Conclusions

Although the aim of integrating the gRNA-landing pads and the use of Cas12 for multiplexing in LX6 is yet to be achieved, several steps towards these end goals were met. The gRNA was successfully assembled, as well as the *ALD5* and *GOR1* gRNA-landing pad - the latter which could be considered the major landmark in this thesis. The success in creating the two gRNA-landing pad offers great opportunities. It provides an example that any gene in *S. cerevisiae* can be adapted to be utilized as a gRNA-landing pad by the already existing MoClo system. While the original MoClo kit and many of the kits expanding on it have parts containing homology arms, these are limited to pre-destined integration loci. Using tailed primers as described in this thesis allows for the integration of complex multi-gene construct anywhere in the genome of *S. cerevisiae*. With the tools expanded on in this thesis, developing a *S. cerevisiae* strain that excels in utilizing acetic acid, and subsequently the sustainable feedstock lignocellulosic hydrolysate, remains a promising possibility.

References

[1] C. E. Wyman and B. Yang, "Cellulosic biomass could help meet california's transportation fuel needs," *California Agriculture*, vol. 63, no. 4, pp. 185–190, Oct. 2009, ISSN: 0008-0845. DOI: 10.3733/ca.v063n04p185. [Online]. Available: https://californiaagriculture.org/article/109157 (visited on 05/02/2024).

[2] J. T. Cunha, P. O. Soares, S. L. Baptista, C. E. Costa, and L. Domingues, "Engineered *saccharomyces cerevisiae* for lignocellulosic valorization: A review and perspectives on bioethanol production," *Bioengineered*, vol. 11, no. 1, pp. 883–903, Jan. 1, 2020, ISSN: 2165-5979, 2165-5987. DOI: 10.1080/21655979.2020.1801178. [Online]. Available: https://www.tandfonline.com/doi/full/10.1080/21655979.2020.1801178 (visited on 05/02/2024).

[3] F. A. Castillo Martinez, E. M. Balciunas, J. M. Salgado, J. M. Domínguez González, A. Converti, and R. P. d. S. Oliveira, "Lactic acid properties, applications and production: A review," *Trends in Food Science & Technology*, vol. 30, no. 1, pp. 70–83, Mar. 2013, ISSN: 09242244. DOI: 10.1016/j.tifs.2012.11.007.

[4] E. J. Oh and Y.-S. Jin, "Engineering of *saccharomyces cerevisiae* for efficient fermentation of cellulose," *FEMS Yeast Research*, vol. 20, no. 1, foz089, Feb. 1, 2020, ISSN: 1567-1356, 1567-1364. DOI: 10.1093/femsyr/foz089. [Online]. Available: https://academic.oup.com/femsyr/article/doi/10.1093/femsyr/foz089/5698803 (visited on 05/02/2024).

[5] R. Singh, A. Prakash, B. Balagurumurthy, and T. Bhaskar, *Recent Advances in Thermo-Chemical Conversion of Biomass*. Elsevier, 2015, ISBN: 978-0-444-63289-0. DOI: 10.1016/C2013-0-00403-3. [Online]. Available: https://doi.org/10.1016/B978-0-444-63289-0.00010-7 (visited on 02/15/2024).

[6] H. K. Jeswani, A. Chilvers, and A. Azapagic, "Environmental sustainability of biofuels: A review," *Proceedings of the Royal Society A: Mathematical, Physical and Engineering Sciences*, vol. 476, no. 2243, p. 20 200 351, Nov. 2020, ISSN: 1364-5021, 1471-2946. DOI: 10.1098/rspa.2020.0351. [Online]. Available: https://royalsocietypublishing.org/doi/10.1098/rspa.2020.0351 (visited on 05/02/2024).

[7] A. Mohr and S. Raman, "Lessons from first generation biofuels and implications for the sustainability appraisal of second generation biofuels," *Energy Policy*, vol. 63, pp. 114–122, Dec. 2013, ISSN: 03014215. DOI: 10.1016/j.enpol.2013.08.033. [Online]. Available: https://linkinghub.elsevier.com/retrieve/pii/S0301421513008264 (visited on 05/02/2024).

[8] E. W. Qian, "Pretreatment and saccharification of lignocellulosic biomass," in *Research Approaches to Sustainable Biomass Systems*, Elsevier, 2014, pp. 181–204, ISBN: 978-0-12-404609-2. DOI: 10.1016/B978-0-12-404609-2.00007-6. [Online]. Available: https://linkinghub.elsevier.com/retrieve/pii/B9780124046092000076 (visited on 05/03/2024).

[9] M. P. Almario, L. H. Reyes, and K. C. Kao, "Evolutionary engineering of *saccharomyces cerevisiae* for enhanced tolerance to hydrolysates of lignocellulosic biomass," *Biotechnology and Bioengineering*, vol. 110, no. 10, pp. 2616–2623, Oct. 2013, ISSN: 0006-3592, 1097-0290. DOI: 10.1002/bit.24938. [Online]. Available: https://onlinelibrary.wiley.com/doi/10.1002/bit.24938 (visited on 05/03/2024).

[10] A. Eliasson Lantz, K. Gernaey, C. Franzén, and L. Olsson, "Online monitoring of fermentation processes in lignocelluloses-to-bioalcohol production," in *Bioalcohol Production*, Elsevier, 2010, p. 317, ISBN: 978-1-84569-510-1. DOI: 10.1533/9781845699611.4.315. [Online]. Available: https://linkinghub.elsevier.com/retrieve/pii/B9781845695101500128 (visited on 05/03/2024).

[11] N. Guaragnella and M. Bettiga, "Acetic acid stress in budding yeast: From molecular mechanisms to applications," *Yeast*, vol. 38, no. 7, pp. 391–400, Jul. 2021, ISSN: 0749-503X, 1097-0061. DOI: 10.1002/yea.3651. [Online]. Available: https://onlinelibrary.wiley.com/doi/10.1002/yea.3651 (visited on 05/06/2024).

[12] M. Fernández-Niño, S. Pulido, D. Stefanoska, *et al.*, "Identification of novel genes involved in acetic acid tolerance of *Saccharomyces cerevisiae* using pooled-segregant RNA sequencing," *FEMS Yeast Research*, vol. 18, no. 8, Dec. 1, 2018, ISSN: 1567-1364. DOI: 10.1093/femsyr/foy100.

[13] G. Vanmarcke, M. M. Demeke, M. R. Foulquié-Moreno, and J. M. Thevelein, "Identification of the major fermentation inhibitors of recombinant 2g yeasts in diverse lignocellulose hydrolysates," *Biotechnology for Biofuels*, vol. 14, no. 1, p. 92, Dec. 2021, ISSN: 1754-6834. DOI: 10.1186/s13068-021-01935-9. [Online]. Available: https://biotechnologyforbiofuels.biomedcentral.com/articles/10.1186/s13068-021-01935-9 (visited on 06/07/2024).

[14] S. Swinnen, M. Fernández-Niño, D. González-Ramos, A. J. A. Van Maris, and E. Nevoigt, "The fraction of cells that resume growth after acetic acid addition is a strain-dependent parameter of acetic acid tolerance in *saccharomyces cerevisiae*," *FEMS Yeast Research*, vol. 14, no. 4, pp. 642–653, Jun. 2014, ISSN: 15671356. DOI: 10.1111/1567-1364.12151. [Online]. Available: https://academic.oup.com/femsyr/article-lookup/doi/10.1111/1567-1364.12151 (visited on 04/15/2024).

[15] X. Zhang, J. G. Nijland, and A. J. M. Driessen, "Combined roles of exporters in acetic acid tolerance in *Saccharomyces cerevisiae*," *Biotechnology for Biofuels and Bioproducts*, vol. 15, no. 1, p. 67, Dec. 2022, ISSN: 2731-3654. DOI: 10.1186/s13068-022-02164-4. [Online]. Available: https://biotechnologyforbiofuels.biomedcentral.com/articles/10.1186/s13068-022-02164-4 (visited on 05/14/2024).

[16] M. Palma, J. F. Guerreiro, and I. Sá-Correia, "Adaptive response and tolerance to acetic acid in *Saccharomyces cerevisiae* and zygosaccharomyces bailii: A physiological genomics perspective," *Frontiers in Microbiology*, vol. 9, p. 274, Feb. 21, 2018, ISSN: 1664-302X. DOI: 10.3389/fmicb.2018.00274. [Online]. Available: http://journal.frontiersin.org/article/10.3389/fmicb.2018.00274/full (visited on 06/07/2024).

[17] F. Saint-Prix, L. Bönquist, and S. Dequin, "Functional analysis of the ALD gene family of *Saccharomyces cerevisiae* during anaerobic growth on glucose: The NADP+-dependent ald6p and ald5p isoforms play a major role in acetate formation," *Microbiology*, vol. 150, no. 7, pp. 2209–2220, Jul. 1, 2004, ISSN: 1350-0872. DOI: 10.1099/mic.0.26999-0.

[18] "Allele: Ald5-," Saccharomyces Genome Database. (), [Online]. Available: https://www.yeastgenome.org/allele/S000281551 (visited on 06/17/2024).

[19] J. A. Diderich, L. M. Raamsdonk, A. L. Kruckeberg, J. A. Berden, and K. Van Dam, "Physiological properties of *saccharomyces cerevisiae* from which hexokinase II has been deleted," *Applied and Environmental Microbiology*, vol. 67, no. 4, pp. 1587–1593, Apr. 2001, ISSN: 0099-2240, 1098-5336. DOI: 10.1128/AEM.67.4.1587-1593.2001. [Online]. Available: https://journals.asm.org/doi/10.1128/AEM.67.4.1587-1593.2001 (visited on 05/06/2024).

[20] I. Papapetridis, M. D. Verhoeven, S. J. Wiersma, M. Goudriaan, A. J. A. Van Maris, and J. T. Pronk, "Laboratory evolution for forced glucose-xylose co-consumption enables identification of mutations that improve mixed-sugar fermentation by xylose-fermenting *Saccharomyces cerevisiae*," *FEMS Yeast Research*, vol. 18, no. 6, Sep. 1, 2018, ISSN: 1567-1364. DOI: 10.1093/femsyr/foy056. [Online]. Available: https://academic.oup.com/femsyr/article/doi/10.1093/femsyr/foy056/4996351 (visited on 05/06/2024).

[21] L. Galdieri, S. Mehrotra, S. Yu, and A. Vancura, "Transcriptional regulation in yeast during diauxic shift and stationary phase," *OMICS: A Journal of Integrative Biology*, vol. 14, no. 6, pp. 629–638, Dec. 2010, ISSN: 1536-2310, 1557-8100. DOI: 10.1089/omi.2010.0069. [Online]. Available: http://www.liebertpub.com/doi/10.1089/omi.2010.0069 (visited on 05/06/2024).

[22] S. Yadav, T. A. Mody, A. Sharma, and A. K. Bachhawat, "A genetic screen to identify genes influencing the secondary redox couple NADPH/NADP+ in the yeast *saccharomyces cerevisiae*," *G3 Genes|Genomes|Genetics*, vol. 10, no. 1, pp. 371–378, Jan. 1, 2020, ISSN: 2160-1836. DOI: 10.1534/g3.119.400606. [Online]. Available: https://academic.oup.com/g3journal/article/10/1/371/6020317 (visited on 05/06/2024).

[23] E. Rintala, J. Pitkänen, M. Vehkomäki, M. Penttilä, and L. Ruohonen, "The ORF *YNL274c* (*GOR1*) codes for glyoxylate reductase in *saccharomyces cerevisiae*," *Yeast*, vol. 24, no. 2, pp. 129–136, Feb. 2007, ISSN: 0749-503X, 1097-0061. DOI: 10.1002/yea.1434. [Online]. Available: https://onlinelibrary.wiley.com/doi/10.1002/yea.1434 (visited on 05/06/2024).

[24] M. Asakura, T. Okuno, and Y. Takano, "Multiple contributions of peroxisomal metabolic function to fungal pathogenicity in *Colletotrichum lagenarium*," *Applied and Environmental Microbiology*, vol. 72, no. 9, pp. 6345–6354, Sep. 2006, ISSN: 0099-2240, 1098-5336. DOI: 10.1128/AEM.00988-06. [Online]. Available: https://journals.asm.org/doi/10.1128/AEM.00988-06 (visited on 05/14/2024).

[25] I. Gostimskaya, "CRISPR–cas9: A history of its discovery and ethical considerations of its use in genome editing," *Biochemistry (Moscow)*, vol. 87, no. 8, pp. 777–788, Aug. 2022, ISSN: 0006-2979, 1608-3040. DOI: 10.1134/S0006297922080090. [Online]. Available: https://link.springer.com/10.1134/S0006297922080090 (visited on 06/07/2024).

[26] F. Yan, W. Wang, and J. Zhang, "CRISPR-cas12 and cas13: The lesser known siblings of CRISPR-cas9," *Cell Biology and Toxicology*, vol. 35, no. 6, pp. 489–492, Dec. 2019, ISSN: 0742-2091, 1573-6822. DOI: 10.1007/s10565-019-09489-1. [Online]. Available: http://link.springer.com/10.1007/s10565-019-09489-1 (visited on 05/07/2024).

[27] J. Z. Jacobs, K. M. Ciccaglione, V. Tournier, and M. Zaratiegui, "Implementation of the CRISPR-cas9 system in fission yeast," *Nature Communications*, vol. 5, no. 1, p. 5344, Oct. 29, 2014, ISSN: 2041-1723. DOI: 10.1038/ncomms6344. [Online]. Available: https://www.nature.com/articles/ncomms6344 (visited on 05/07/2024).

[28] C. Xue and E. C. Greene, "DNA repair pathway choices in CRISPR-cas9-mediated genome editing," *Trends in Genetics*, vol. 37, no. 7, pp. 639–656, Jul. 2021, ISSN: 01689525. DOI: 10.1016/j.tig.2021.02.008. [Online]. Available: https://linkinghub.elsevier.com/retrieve/pii/S0168952521000536 (visited on 05/07/2024).

[29] D. Kim, J. Kim, J. K. Hur, K. W. Been, S.-h. Yoon, and J.-S. Kim, "Genome-wide analysis reveals specificities of cpf1 endonucleases in human cells," *Nature Biotechnology*, vol. 34, no. 8, pp. 863–868, Aug. 2016, ISSN: 1087-0156, 1546-1696. DOI: 10.1038/nbt.3609. [Online]. Available: https://www.nature.com/articles/nbt.3609 (visited on 05/07/2024).

[30] Y. Tang and Y. Fu, "Class 2 CRISPR/cas: An expanding biotechnology toolbox for and beyond genome editing," *Cell & Bioscience*, vol. 8, no. 1, p. 59, Dec. 2018, ISSN: 2045-3701. DOI: 10.1186/s13578-018-0255-x. [Online]. Available: https://cellandbioscience.biomedcentral.com/articles/10.1186/s13578-018-0255-x (visited on 05/07/2024).

[31] M. Meliawati, C. Schilling, and J. Schmid, "Recent advances of cas12a applications in bacteria," *Applied Microbiology and Biotechnology*, vol. 105, no. 8, pp. 2981–2990, Apr. 2021, ISSN: 0175-7598, 1432-0614. DOI: 10.1007/s00253-021-11243-9. [Online]. Available: http://link.springer.com/10.1007/s00253-021-11243-9 (visited on 06/07/2024).

[32] X. Ao, Y. Yao, T. Li, *et al.*, "A multiplex genome editing method for escherichia coli based on CRISPR-cas12a," *Frontiers in Microbiology*, vol. 9, p. 2307, Oct. 9, 2018, ISSN: 1664-302X. DOI: 10.3389/fmicb.2018.02307. [Online]. Available: https://www.frontiersin.org/article/10.3389/fmicb.2018.02307/full (visited on 06/07/2024).

[33] S. Kim, D. Kim, S. W. Cho, J. Kim, and J.-S. Kim, "Highly efficient RNA-guided genome editing in human cells via delivery of purified cas9 ribonucleoproteins," *Genome Research*, vol. 24, no. 6, pp. 1012–1019, Jun. 2014, ISSN: 1088-9051. DOI: 10.1101/gr.171322.113. [Online]. Available: http://genome.cshlp.org/lookup/doi/10.1101/gr.171322.113 (visited on 05/07/2024).

[34] M. Mormino, I. Lenitz, V. Siewers, and Y. Nygård, "Identification of acetic acid sensitive strains through biosensor-based screening of a *Saccharomyces cerevisiae* CRISPRi library," *Microbial Cell Factories*, vol. 21, no. 1, p. 214, Oct. 15, 2022, ISSN: 1475-2859. DOI: 10.1186/s12934-022-01938-7.

[35] S. Swinnen, S. F. Henriques, R. Shrestha, P.-W. Ho, I. Sá-Correia, and E. Nevoigt, "Improvement of yeast tolerance to acetic acid through haa1 transcription factor engineering: Towards the underlying mechanisms," *Microbial Cell Factories*, vol. 16, no. 1, p. 7, Dec. 2017, ISSN: 1475-2859. DOI: 10.1186/s12934-016-0621-5. [Online]. Available: http://microbialcellfactories.biomedcentral.com/articles/10.1186/s12934-016-0621-5 (visited on 04/23/2024).

[36] B. Choi, A. Tafur Rangel, E. J. Kerkhoven, and Y. Nygård, "Engineering of *Saccharomyces cerevisiae* for enhanced metabolic robustness and l-lactic acid production from lignocellulosic biomass," *Metabolic Engineering*, vol. 84, pp. 23–33, Jul. 2024, ISSN: 10967176. DOI: 10.1016/j.ymben.2024.05.003. [Online]. Available: https://linkinghub.elsevier.com/retrieve/pii/S1096717624000697 (visited on 05/30/2024).

[37] J. O. Westman, N. Bonander, M. J. Taherzadeh, and C. J. Franzén, "Improved sugar co-utilisation by encapsulation of a recombinant *Saccharomyces cerevisiae* strain in alginate-chitosan capsules," *Biotechnology for Biofuels*, vol. 7, no. 1, p. 102, Dec. 2014, ISSN: 1754-6834. DOI: 10.1186/1754-6834-7-102. [Online]. Available: https://biotechnologyforbiofuels.biomedcentral.com/articles/10.1186/1754-6834-7-102 (visited on 05/08/2024).

[38] B. A. Rabe and C. Cepko, *A simple enhancement for gibson isothermal assembly*, Jun. 15, 2020. DOI: 10.1101/2020.06.14.150979. [Online]. Available: http://biorxiv.org/lookup/doi/10.1101/2020.06.14.150979 (visited on 05/27/2024).

[39] L. Torello Pianale and L. Olsson, "*Sc* EnSor kit for *saccharomyces cerevisiae* engineering and biosensor-driven investigation of the intracellular environment," *ACS Synthetic Biology*, vol. 12, no. 8, pp. 2493–2497, Aug. 18, 2023, ISSN: 2161-5063, 2161-5063. DOI: 10.1021/acssynbio.3c00124. [Online]. Available: https://pubs.acs.org/doi/10.1021/acssynbio.3c00124 (visited on 05/17/2024).

[40] J. R. Sayers and F. Eckstein, "A single-strand specific endonuclease activity copurifies with overexpressed t5 d15 exonuclease," *Nucleic Acids Research*, vol. 19, no. 15, pp. 4127–4132, Aug. 11, 1991, ISSN: 0305-1048. DOI: 10.1093/nar/19.15.4127.

[41] R. Verwaal, N. Buiting-Wiessenhaan, S. Dalhuijsen, and J. A. Roubos, "CRISPR/cpf1 enables fast and simple genome editing of *Saccharomyces cerevisiae*," *Yeast*, vol. 35, no. 2, pp. 201–211, Feb. 12, 2018, ISSN: 0749-503X. DOI: 10.1002/yea.3278.

[42] J. C. Utomo, C. L. Hodgins, and D.-K. Ro, "Multiplex genome editing in yeast by CRISPR/cas9 – a potent and agile tool to reconstruct complex metabolic pathways," *Frontiers in Plant Science*, vol. 12, p. 719 148, Aug. 5, 2021, ISSN: 1664-462X. DOI: 10.3389/fpls.2021.719148. [Online]. Available: https://www.frontiersin.org/articles/10.3389/fpls.2021.719148/full (visited on 05/28/2024).

[43] L. Zhang, J. A. Zuris, R. Viswanathan, *et al.*, "AsCas12a ultra nuclease facilitates the rapid generation of therapeutic cell medicines," *Nature Communications*, vol. 12, no. 1, p. 3908, Jun. 23, 2021, ISSN: 2041-1723. DOI: 10.1038/s41467-021-24017-8. [Online]. Available: https://www.nature.com/articles/s41467-021-24017-8 (visited on 05/28/2024).

[44] K. S. Ghanta and C. C. Mello, "Melting dsDNA donor molecules greatly improves precision genome editing in caenorhabditis elegans," *Genetics*, vol. 216, no. 3, pp. 643–650, Nov. 2020, ISSN: 1943-2631. DOI: 10.1534/genetics.120.303564.

[45] C. C. Mello, J. M. Kramer, D. Stinchcomb, and V. Ambros, "Efficient gene transfer in c.elegans: Extrachromosomal maintenance and integration of transforming sequences," *The EMBO journal*, vol. 10, no. 12, pp. 3959–3970, Dec. 1991, ISSN: 0261-4189. DOI: 10.1002/j.1460-2075.1991.tb04966.x.

[46] S. A. Oh, K. Senger, S. Madireddi, *et al.*, "High-efficiency nonviral CRISPR/cas9-mediated gene editing of human t cells using plasmid donor DNA," *Journal of Experimental Medicine*, vol. 219, no. 5, e20211530, May 2, 2022, ISSN: 0022-1007, 1540-9538. DOI: 10.1084/jem.20211530. [Online]. Available: https://rupress.org/jem/article/219/5/e20211530/213176/High-efficiency-nonviral-CRISPR-Cas9-mediated-gene (visited on 05/28/2024).

[47] R. Singh, S. Chandel, A. Ghosh, *et al.*, "Easy efficient HDR-based targeted knock-in in *saccharomyces cerevisiae* genome using CRISPR-cas9 system," *Bioengineered*, vol. 13, no. 6, pp. 14 857–14 871, Jun. 1, 2022, ISSN: 2165-5979, 2165-5987. DOI: 10.1080/21655979.2022.2162667. [Online]. Available: https://www.tandfonline.com/doi/full/10.1080/21655979.2022.2162667 (visited on 05/28/2024).

[48] J. Ding, J. Bierma, M. R. Smith, *et al.*, "Acetic acid inhibits nutrient uptake in *Saccharomyces cerevisiae*: Auxotrophy confounds the use of yeast deletion libraries for strain improvement," *Applied Microbiology and Biotechnology*, vol. 97, no. 16, pp. 7405–7416, Aug. 2013, ISSN: 0175-7598, 1432-0614. DOI: 10.1007/s00253-013-5071-y. [Online]. Available: http://link.springer.com/10.1007/s00253-013-5071-y (visited on 05/29/2024).

[49] E. Cámara, I. Lenitz, and Y. Nygård, "A CRISPR activation and interference toolkit for industrial *Saccharomyces cerevisiae* strain KE6-12," *Scientific Reports*, vol. 10, no. 1, p. 14 605, Sep. 3, 2020, ISSN: 2045-2322. DOI: 10.1038/s41598-020-71648-w. [Online]. Available: https://www.nature.com/articles/s41598-020-71648-w (visited on 05/10/2024).

[50] M. E. Lee, W. C. DeLoache, B. Cervantes, and J. E. Dueber, "A highly characterized yeast toolkit for modular, multipart assembly," *ACS Synthetic Biology*, vol. 4, no. 9, pp. 975–986, Sep. 18, 2015, ISSN: 2161-5063, 2161-5063. DOI: 10.1021/sb500366v. [Online]. Available: https://pubs.acs.org/doi/10.1021/sb500366v (visited on 05/17/2024).

A

Appendix

Table 7: List of all plasmids used in this thesis.

Plasmids

Plasmid name	Genotype	Origin
pMM4_14L	pH- and acetic acid biosensor expressing *sfpHluorin*, *mCherry* and *mTurquoise2*. Flanked by HOp homology arms	Nygård paper [34]
pMM4_14U	pMM4_14LΔ::*URA3* Acetic acid biosensor expressing *mCherry* and *mTurquoise2*. Flanked by *URA3* homology arms	Developed by Arne Peetermans for this study
YN2_1_Cas9_gRNA	Backbone Cas9 *GFP*-dropout cassette AgTEFp-*KanR*-AgTEFt	Cámara paper [49]
YN2_1 HOi	YN2_1_Cas9_gRNA *GFP*Δ::sgRNA targetting HO ORF	This study
YN2_1 IL50	YN2_1_Cas9_gRNA *GFP*Δ::sgRNA targetting HOp	This study
YN2_1_URA3	YN2_1_Cas9_gRNA *GFP*Δ::sgRNA targetting *URA3*	Developed by Arne Peetermans for this study
crRNA_Cpf1_backbone	Backbone crRNA for Cas12 *GFP*-dropout cassette AgTEFp-*KanR*-AgTEFt AmpRp-*AmpR*-AmpRt	This study, ordered from Addgene
crRNA_Cpf1_GOR1	crRNA_Cpf1_backbone *GFP*Δ::sgRNA targetting *GOR1*	This study
crRNA_Cpf1_HXK2	crRNA_Cpf1_backbone *GFP*Δ::sgRNA targetting *HXK2*	This study
crRNA_Cpf1_ALD5	crRNA_Cpf1_backbone *GFP*Δ::sgRNA targetting *ALD5*	This study
crRNA_Cpf1_array	crRNA_Cpf1_backbone *GFP*Δ::sgRNA-array targetting all three deletion-targets	This study
pCSN067	Backbone LbCpf1 (Cas12) TEFp-*KanR*-TEFt	Verwaal paper [41]
pYTK017	MoClo part containing ScRPL18B promoter	MoClo paper [50]

Plasmid name	**Plasmid features**	**Origin**
LT0_4_ymYPET	Precursor to *Sc*EnSor kit. Plasmid containing *ymYPET*	Lab plasmid collection. Developed by Luca Torello Pinale and Lisbeth Olsson [39]
pYTK052	MoClo part containing ScSSA1 terminator	MoClo paper [50]
pYTK067	MoClo part containing connector	MoClo paper [50]
pYTK074	MoClo part containing *URA3*	MoClo paper [50]
pYTK083	MoClo part *RFP* and AmpR *URA3*	MoClo paper [50]

Table 8: List of all primers used in this project.

Primer name	**Primer sequence**	**Description**
AP4_1.1	gggttccctttttataattggcggaact tctcttgttttgtgaccacttccttcatc ggtatcttcgctata	Forward TEF1p amplification. Homology with HO integration site.
AP12_TEF1pR_Gibson	tgtacggcagagggcgacattttgtaat taaaacttagattagattgctatgcttt ctttctaa	Reverse TEF1p amplification. Homology with *ACS1*.
AP11_ACS1FW	atctaatctaagttttaattacaaaatg tcgccctctgccgt	Forward *ACS1* amplification. Homology with TEF1p.
AP14_ACS1ORF_REV	cgatttcaattcaattcaatttacaact tgaccgaatcaa	Reverse *ACS1* amplification. Homology with PGK1t.
AP4_3.1	Tgtcaaaccctggcattgttagacatct aattgattcggtcaagttgtaacgatag atcaatttttttctttctctttcccca tcctttacgctaaaat	Forward PGK1t amplification. Homology with *ACS1*.
AP4_3.2	atatttcaagatctcttggtatgtcagc tactgtgacgaccaggtcagcttaacga acgcagaattttcgagt	Reverse PGK1t amplification. Homology with HO integration site.
AP2_sgRNA_HOi_FW	GACTtacgactgtaatgttgctgg	Oligo gRNA targetting HO orf.
AP2_sgRNA_HOi_RV	AAACcagcaacattacagtcgta	Oligo gRNA targetting HO orf.
IL50_sgHO_YN2-1_fw	gactgctccagcattatagcatgc	Oligo gRNA targetting HOp.
IL50_sgHO_YN2-1_rev	aaacgcatgctataatgctggagc	Oligo gRNA targetting HOp.
AP19_gRNA_URA3.2_FW	gactgggtcaacagtatagaaccg	Oligo gRNA targetting *URA3*.
AP19_gRNA_URA3.2_RV	aaaccggttctatactgttgaccc	Oligo gRNA targetting *URA3*.
AP35_GOR1_Left_FW	accctagagaccgaattcGGCTTAG ATTCATTGGGCCAG	Forward amplification of the left GOR1 homology arm.
AP25_GOR1_LeftHA_REV	ggtctcccgttgaattcGACACCAG CTTCCTTCCGAAG	Reverse amplification of the left GOR1 homology arm.
AP26_GOR1_RightHA_FW	ggtctcagagtaagcttCTTCTCCT CTTCTTGCTCGT	Forward amplification of the right GOR1 homology arm.
AP36_GOR1_Right_REV	atcggagagaccaagcttGGGAAGC AATTCATACAGGGC	Reverse amplification of the right GOR1 homology arm.
AP33_HXK2_Left_FW	accctagagaccgaattcCCTCGCA CATTGGTACCTAG	Forward amplification of the left HXK2 homology arm.
AP27_HXK2_LeftHA_REV	ggtctcaccctgaattcCCTCGCAC ATTGGTACCTAG	Reverse amplification of the left HXK2 homology arm.
AP28_HXK2_RightHA_FW	ggtctcagagtaagcttACCCAATC AAGATTGTTCCT	Forward amplification of the right HXK2 homology arm.
AP34_HXK2_Right_REV	atcggagagaccaagcttTAGAGGA AGTGTAGAGAGGG	Reverse amplification of the right HXK2 homology arm.
AP31_ALD5_Left_FW	accctagagaccgaattcTAGCAAG GGCCTAATGGTACG	Forward amplification of the left ALD5 homology arm.
AP29_ALD5_LeftHA_REV	ggtctcccgttgaattcCTGTCTTA ACCACGTTTGATG	Reverse amplification of the left ALD5 homology arm.
AP30_ALD5_RightHA_FW	ggtctcagagtaagcttAGTAACTC AGGCCCGAGTTG	Forward amplification of the right ALD5 homology arm
AP32_ALD5_Right_REV	atcggagagaccaagcttGGTGATG AATACTCGCCGAG	Reverse amplification of the right ALD5 homology arm
AP21_BS_URA3_DDNA _ST_FW	aacaaaaacctgcaggaaacgaagataa taacgatggcttcttatctcac	Amplify pMM4_14 to replace HO homology with *URA3* homology.

AP21_BS_URA3_DDNA_ST_RV	tagtatacatgcatttacttataatacagagcagtacttcaaccattag	Amplify pMM4_14 to remove *URA3* and replace HO homology with *URA3* homology.
HXK2_gRNA_P1_FW	ccctaatttctactaagtgtagatcggctggactcaaacctcacgctg	Construct sgRNA targetting *HXK2* in sgRNA-array.
HXK2_gRNA_P1_REV	gtgaggtttgagtccagccgatctacacttagtagaaatt	Construct sgRNA targetting *HXK2* in sgRNA-array.
ALD5_gRNA_P2_FW	aatttctactaagtgtagatgtgcgcgcggtgacgtcgct	Construct sgRNA targetting *ALD5* in sgRNA-array.
ALD5_gRNA_P2_REV	actcagcgacgtcaccgcgcgcacatctacacttagtagaaattcagc	Construct sgRNA targetting *ALD5* in sgRNA-array.
GOR1_gRNA_P3(end)_FW	gagtaatttctactaagtgtagatagagagattgaagccgtttg	Construct sgRNA targetting *GOR1* in sgRNA-array.
GOR1_gRNA_P3(end)_REV	cgttcaaacggcttcaatctctctatctacacttagtagaaatt	Construct sgRNA targetting *GOR1* in sgRNA-array.
HXK2_gRNA_single_FW	ccctaatttctactaagtgtagatcggctggactcaaacctcacg	Construct sgRNA targetting *HXK2*.
HXK2_gRNA_single_REV	cgttgtgaggtttgagtccagccgatctacacttagtagaaatt	Construct sgRNA targetting *HXK2*.
ALD5_gRNA_single_FW	ccctaatttctactaagtgtagatgtgcgcgcggtgacgtcgct	Construct sgRNA targetting *ALD5*.
ALD5_gRNA_single_REV	cgttagcgacgtcaccgcgcgcacatctacacttagtagaaat	Construct sgRNA targetting *ALD5*.
GOR1_gRNA_single_FW	ccctaatttctactaagtgtagatagagagattgaagccgtttg	Construct sgRNA targetting *GOR1*.
GOR1_gRNA_single_REV	cgttcaaacggcttcaatctctctatctacacttagtagaaatt	Construct sgRNA targetting *GOR1*.
AP1_RET1p_RV	gcaagtagtattcgacctgga	Check for integration of biosensor. Pairs with AP37_URA3_OUTSIDE_FW.
AP37_URA3_OUTSIDE_FW	ggagcacagacttagattgg	Check for integration of biosensor. Pairs with AP1_RET1p_RV.
AP37_URA3_OUTSIDE_REV	ggttctggcgaggtattgg	Check for integration of biosensor. Pairs with AP38_SSA1t_REV.
AP38_SSA1t_REV	ccaattggtgcggcaattga	Check for integration of biosensor. Pairs with AP37_URA3_OUTSIDE_REV
AP43_URA3_LP_FW	cgttacagaaaagcaggctgg	Check for URA3 in landing pad. Pairs with AP44.
AP48_ColE1_left_check_fw	tgtcgggtttcgccacctct	Check for *E. coli* ori in landing pad. Pairs with AP51.
AP44_YPET_LP_REV	caccggtgaacaattcttcgc	Check for *ymYPET* in landing pad. Pairs with AP43.
AP51_AmpR_right_check_rv	agccctcccgtatcgtagtt	Check for *AmpR* in landing pad. Pairs with AP48.
AP42_CPF1(Verwaal)_FW	gagcgcgcgtaatacgact	Forward amplification of Cas12 from pCSN067.
AP42_CPF1(Verwaal)_REV	acctgcagcgtacgaagctt	Reverse amplification of Cas12 from pCSN067.

AP41_crRNA(Cpf1)_FW	ctcatacacgagttgagaccg	Forward amplification of sgRNA plasmids. Pairs with other AP41.
AP41_crRNA(Cpf1)_REV	aactgtactgcagtgcacta	Forward amplification of sgRNA plasmids. Pairs with other AP41.

Protocol 1: NEB Q5 PCR

In a PCR tube add the following:

- 5µL ..... 5X Q5 Reaction Buffer
- 0.5µL ..... 10 mM dNTPS
- 1.25 µL ..... Forward Primer
- 1.25 µL ..... Reverse Primer
- 0.5-1.25 µL ..... Template DNA
- 0.25µL ..... Q5 High-Fidelity DNA Polymerase
- to 25 µL ..... Nuclease-Free Water

Thermocycling conditions for Q5PCR:

1. Initial Denaturation:
   - 98 °C ..... 30 seconds
2. 30 Cycles of:
   - 98 °C ..... 5-10 seconds
   - 50-72 °C ..... 10-30 seconds
   - 72 °C ..... 20-30 seconds/kb
3. Final extension:
   - 72 ° ..... 2 minutes
4. Hold:
   - 4-10 °C ..... until use

Protocol 2: NEB Taq PCR

In a PCR tube add the following:

- 5µL ..... 10X Standard *Taq* Reaction Buffer
- 0.5µL ..... 10 mM dNTPS
- 0.5 µL ..... Forward Primer
- 0.5 µL ..... Reverse Primer
- 0.5-1.25 µL ..... Template DNA
- 0.125µL ..... *Taq* DNA polymerase
- to 25 µL ..... Nuclease-Free Water

Thermocycling conditions for *Taq* PCR:

1. Initial Denaturation:
   - 95 °C ..... 30 seconds
2. 30 Cycles of:
   - 95 °C ..... 15-30 seconds
   - 45-68 °C ..... 15-60 seconds
   - 68 °C ..... 1 minute/kb
3. Final extension:
   - 68 ° ..... 5 minutes
4. Hold
   - 4-10 °C ..... until use

Protocol 3: Thermo fisher Phire Plant PCR (Colony PCR)

In a PCR tube add the following:

- 10 µL ..... 2X Phire Plant PCR Buffer
- 2.5 µL ..... Forward Primer
- 2.5 µL ..... Reverse Primer
- 0.4 µL ..... Phire Hot Start II DNA Polymerase
- Swab sample ..... Bacteria or Yeast colony

Thermocycling conditions for colony PCR:

1. Initial Denaturation:
   - 98 °C ..... 5 min
2. 40 Cycles of:
   - 98 °C ..... 5 seconds
   - 62-72 °C ..... 5 seconds
   - 72 °C ..... 20 seconds/kb
3. Final extension:
   - 72 ° ..... 5 minutes
4. Hold
   - 4-10 °C ..... until use

Protocol 4: Gel electrophoresis protocol

Making the agarose gel:

- Add 4g of agarose to a 400mL microwavable flask.
- Fill with 0.5xTAE buffer.
- Microwave until agarose has dissolved.
- Keep in 65 °C until use.

Solidify the gel by mixing 1.5 µL SYBR safe per 50mL of agarose gel in a 50mL falcoln tube and pouring it out on a casting tray.

Making the samples For each sample one wishes to analyze, in the wells add:

- 7 µL water
- 3 µL DNA sample
- 2 µL load buffer

Run the gels at 85-95V for 25-35 minutes. Analyze using UV light-equipped visualization device.

Protocol 5: Restriction of plasmid

In a 50 µl PCR tube, add the following:

1. 5 µl NEBuffer 3.1
2. 1 µg plasmid
3. 10U restriction enzyme (Generally 0.5-1 µl)
4. to 50 µl, Nuclease-free water

Place in thermocycler and run at:

1. 37 °C for 2h to 12h.
2. Heat-inactivation temperature for R.E. Generally 65-80 °C - for 20 min.
3. 4 °until use.

Protocol 6: Anneal oligos

If inserting single-target oligos, in a 50 µl PCR tube add the following:

1. 9 µl 100 µM FW oligo
2. 9 µl 100 µM REV oligo
3. 2 µl T4 DNA ligase buffer (NEB)

Place PCR tube in thermocycler and run it at:

1. 95 °C for 10 minutes
2. 95-4 °C. Decreasing with 1 °C per 15 seconds.

Dilute final solution 1:100 with nuclease-free water.

If inserting multiple-target oligos, such as for the sgRNA-array, in one PCR tube for each oligo add the following:

1. 2.5 µl 10uM oligo. NOTE: Only ONE oligo per PCR tube.
2. 1 µl T4 polynucleotide kinase
3. 5 µl 10x T4 ligase buffer
4. to 50 µl, Nuclease-free water

Place all PCR tubes in a thermocycler and run it at the following settings:

1. 37 °C for 30 min
2. 65 °C for 20 min

Pair matching oligos by adding 25 µl of each into a PCR tube. Put in thermocycler and run at:

1. 95 °C for 5 minutes
2. 95-4 °C. Decreasing with 1 °C per 15 seconds.

Protocol 7: Restriction cloning protocol

In a PCR tube add the following:

1. 2 µl T4 buffer
2. 1 µl T4 ligase
3. 50 ng restricted plasmid
4. 37.5 ng of each oligo. (Roughly 1 µl of each 1:100 oligo pair)
5. to 20 µl, nuclease-free water

Put in thermocycler and run at:

1. 25 °C 2h
2. 65 °C 10 min
3. 4 °C until use

Protocol 8: Electroporation transformation of *E. coli*

1. Chill electroporation cuvette (2 mm), put fresh LB, and DNA samples on ice.
2. Thaw electrocompetent cells on ice.
3. Add 0.5 – 2.5 µl of DNA sample into the competent cells and stay 1 min on ice.
4. Gently transfer competent cells into the cuvettes. Tap the cuvette gently on the counter to move cells to the bottom.
5. Turn on electroporator and set voltage to 2.4kV.
6. Wipe off excess moisture to the cuvette and place cuvette in electroporator.
7. Press "pulse" button on the electroporator to shock cells. Then, remove cuvette from the chamber and immediately add ice-cold LB.
8. Spin down in 200 µL water (4000rpm, 3 min).
9. Plate transformation onto pre-warmed LB-agar plate (190 µl).
10. Dilute the remaining 10 µL with 190 µL water and plate onto another agar plate.
11. Incubate overnight at 37 °C.

Protocol 9: Super Protocol GIETZ transformation

1. Grow cells until O.D ±1
2. Centrifuge for 5 min at 3000rpm
3. Remove supernatans and resuspend the pellet in 1ml 0.1M LiAc
4. Transfer into eppendorf tube
5. Centrifuge 2 min at 3000rpm and remove supernatans
6. Resuspend in 100µl 0.1M LiAc (depending from the amount of transformations, the max volume is 500µl, enough for 10 transformations)
7. 10 min at room temperature
8. Pipet in new eppendorf tube:
   (a) 50µl cells
   (b) 300µl Pli mix (1ml LiAc, 1 ml H2O, 8 ml 3350 PEG 50%)
   (c) 5µl SSDNA (10mg/ml) boiled
   (d) 50µl PCR product or 1µg plasmid DNA
9. vortex 10 sec
10. Incubate 30 min at 42°C in shaking waterbath
11. Centrifuge 2 min at 4000rpm
    if selection on antibiotics medium: include a rescue-period before plating on the antibiotic-containing plates Rescue step: after the heat shock and centrifugation: take the pellet in 1 mL YPD; suspend gently by slowly pipetting up and down. Close the epps and stick them onto a shaking rack at 30°C. Let shake for 3-4 hours; then centrifuge
12. Remove supernatans and resuspend in 500µl sterile H2O
13. Plate out 500µl on selective medium.

Protocol 10: GIETZ protocol 2002 transformation

1. Grow cells until ∼OD 5.8
2. Distribute cells in 1.5 ml eppendorf tubes.
3. Pellet cells (3000rpm, 3 min)
4. Wash with 1 ml 0.1M LiAc.
5. Resuspend in 100 0.1M LiAc.
6. Pellet cells (8000rpm, 3 min).
7. Resuspend in 10 µl boiled salmon sperm, donor DNA, and milli-Q water up to 64 µl.
8. Incubate at room temperature for 30 min.
9. Add 294 µl PEG-LiAc (260 µl (w/v) PEG3350 + 36 µl 1M LiAc).
10. Vortex for 5 seconds. Incubate at room temperature for 30 minutes.
11. Water bath at 42 °C for 15 minutes.
12. Pellet cells (8000 rpm, 3 min).
13. Resuspend in YPD and recover for 3h or plate when using auxotrophic selection.

Protocol 11: NEB Gibson Assembly protocol (E5510)

1. Set up the following reaction on ice:
   - DNA fragments ..... 100 ng
   - Gibson Assembly Master Mix (2X) ..... 10 µl
   - Deoinized Milli-Q water ..... to 20 µl
2. Incubate samples in a thermocycler at 50 °C for 15-60 min.
3. Store samples at -20 °C.

Protocol 12: DNA extraction (LiAc)

1. Pick one yeast colony from the plate or spin down 100-200 µl of liquid yeast culture (OD600=0.4). Suspend cells in 100 µl of 200mM LiAc, 1
2. Incubate for 5 minutes at 70°C.
3. . Add 300µl of 96-100
4. . Spin down DNA and cell debris at 15 000 g for 3 minutes.
5. . Wash pellet with 70
6. . Dissolve pellet in 100 µl of H2O or TE and spin down cell debris for 15 seconds at 15 000 g.
7. . Use 1 µl of supernatant for PCR.

Stock solutions

1. 0.2 M Lithium acetate 1% SDS solution. (LiAc 20,4g/L; SDS 10g/L)
2. Ethanol 96-100 % and 70 %.

Protocol 13: DNA extraction (NaOH)

In an PCR tube add:

- 30 mL 20mM NaOH
- Half a colony *S. cerevisiae*

Heat at 100 °C for 10 min.
Spin down the solution and use 1 µl.

Protocol 14: Golden Gate Assembly protocol

1. Set up assemble reaction as follows:
   - Backbone plasmid ..... 75 ng
   - Inserts ..... 75 ng per insert
   - T4 DNA Ligase buffer (10X) ..... 2 µl
   - T4 DNA Ligase Buffer (10x) ..... 2 uL
   - T4 DNA ligase 2000 U/uL ..... 0.5 uL
   - BsaI-HF-v2 20 U/uL ..... 1.5 uL
   - Nuclease-free water ..... to 20 uL
2. Run thermocycler at 37 °C for 1 min followed by 16 °C for 1 min, 30 times.
   37 °C for 5 min.
   60 °C for 20 min.
   Infinite hold at 4 °C.

DEPARTMENT OF LIFE SCIENCES
CHALMERS UNIVERSITY OF TECHNOLOGY
Gothenburg, Sweden 2024
www.chalmers.se

CHALMERS
UNIVERSITY OF TECHNOLOGY